Radiometric Performance of the Calibration Demonstration System Fourier Transform Spectrometer

David Johnson

January 9, 2014

Acknowledgments

IR Calibration Demonstration System (CDS) Spectrometer

Engineering and Technical:

LaRC: Nurul Abedin, Ashley Alford, Jennifer Allen, Chuck Antill, Dick Bender, Charlie Boyer, Frank Boyer, Rich Cageao, Bill Culliton, Barry Dunn, Glenn Farnsworth, Mick Hartzheim, Ron Huppi, Peter Huynh, Dave Johnson, Cathy Kern, Paul Manhart, Joe McKenney, Johnny Mau, Wade May, Mark Motter, Willie Munden, Ben Nickless, Joe O'Connell, Jim Osmundsen, Irene Pang, Steve Pennington, Tamer Refaat, Don Robinson, Ray Seals, Tory Scola, Tim Shekoski, Katie Smith, Chris Thames, Joe Walker, Tim Wood

GSFC: Ken Blumenstock, Tom Capon, Alex Cramer, Don Jennings, Ken Lee, Brendan McAndrew

Management:

LaRC: Rosemary Baize, Kevin Brown, Jerri Carter, Jim Corliss, Mary Dijoseph, Don Garber, Mike Gazarik, Nicole Hintermeister, Susie Johnston, Alan Little, Bill Luck, Ken Parkinson, Steve Sanford, Jo Sawyer, Don Shick, Dave Young

Science:

Ron Huppi, Don Jennings, Dave Johnson, Marty Mlynczak, Bruce Wielicki

Variable Temperature Blackbody (CORSAIR IIP, SDL)

Engineering:

SDL: Gail Bingham, Harri Latvakoski, Seth Topham, Mike Watson, Mike Wojcik

CDS Overview

- Objective: Demonstrate brightness temperature measurements with an accuracy of 0.1 K (k=3) in a laboratory environment for scene temperatures of 200-320 K from 200 to 2000 cm^{-1} .
- Key Features:
  - 4-port Fourier transform spectrometer (FTS);
  - Input pupil at calibration blackbody aperture, intermediate pupil at FTS cube corner, exit pupil at FTS output.
  - FTS operated in vacuum housing for thermal and acoustic isolation, elimination of atmospheric absorption, and protection of hygroscopic CsI beamsplitter.
  - Include observations of a variable temperature blackbody source to quantify measurement bias over a range of scene temperatures.

CDS Hardware

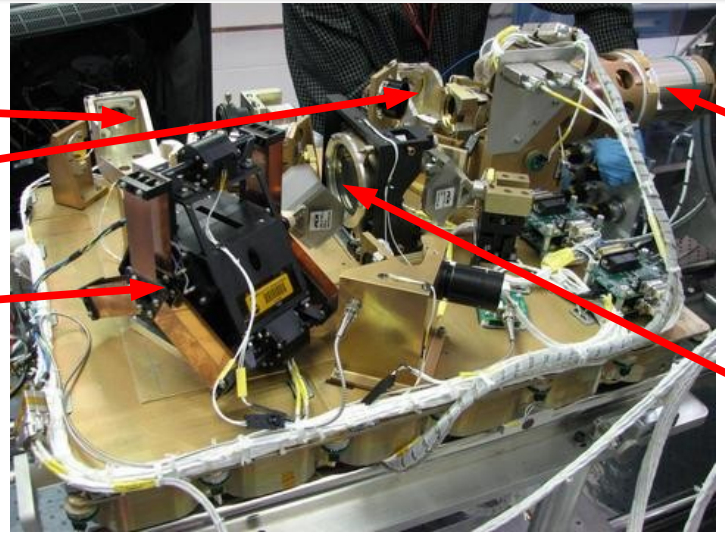

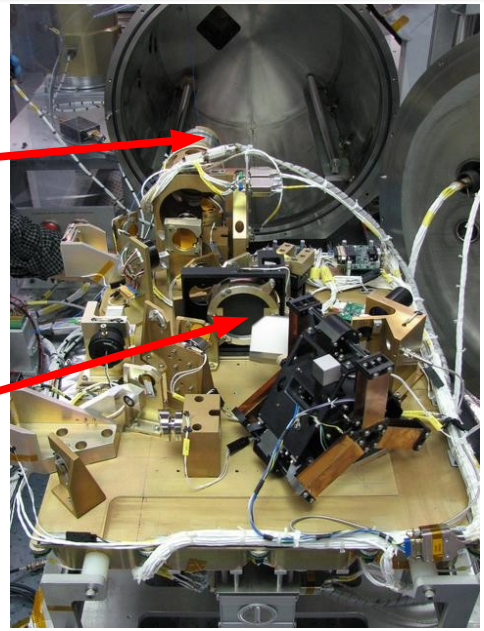

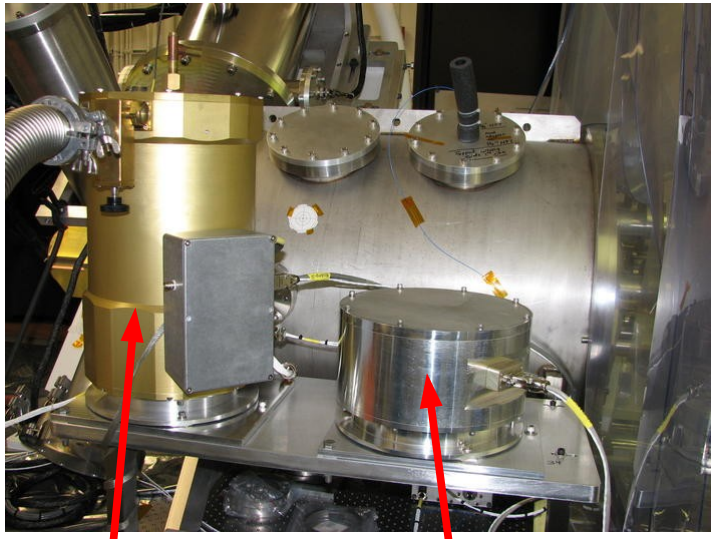

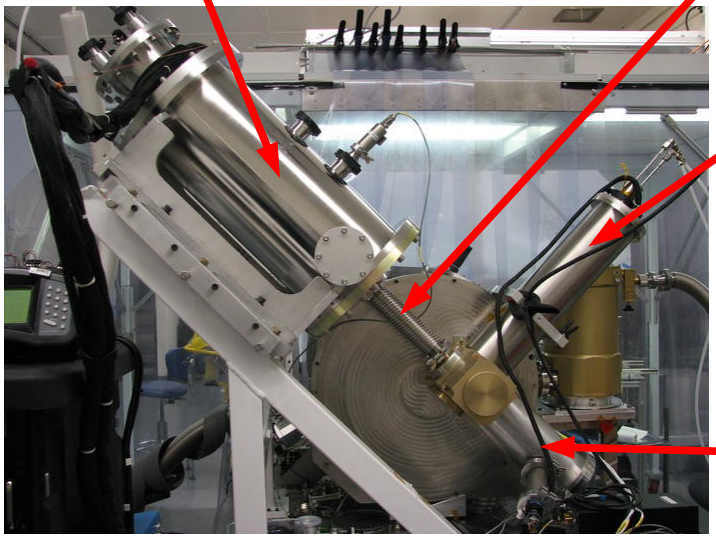

CDS Optical Layout

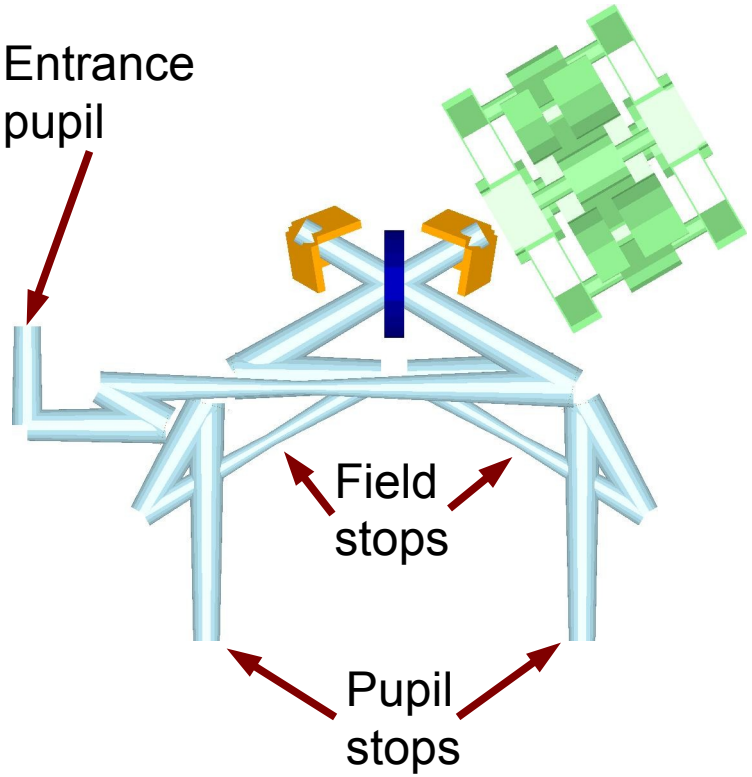

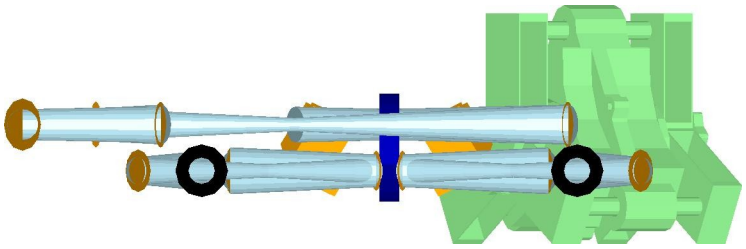

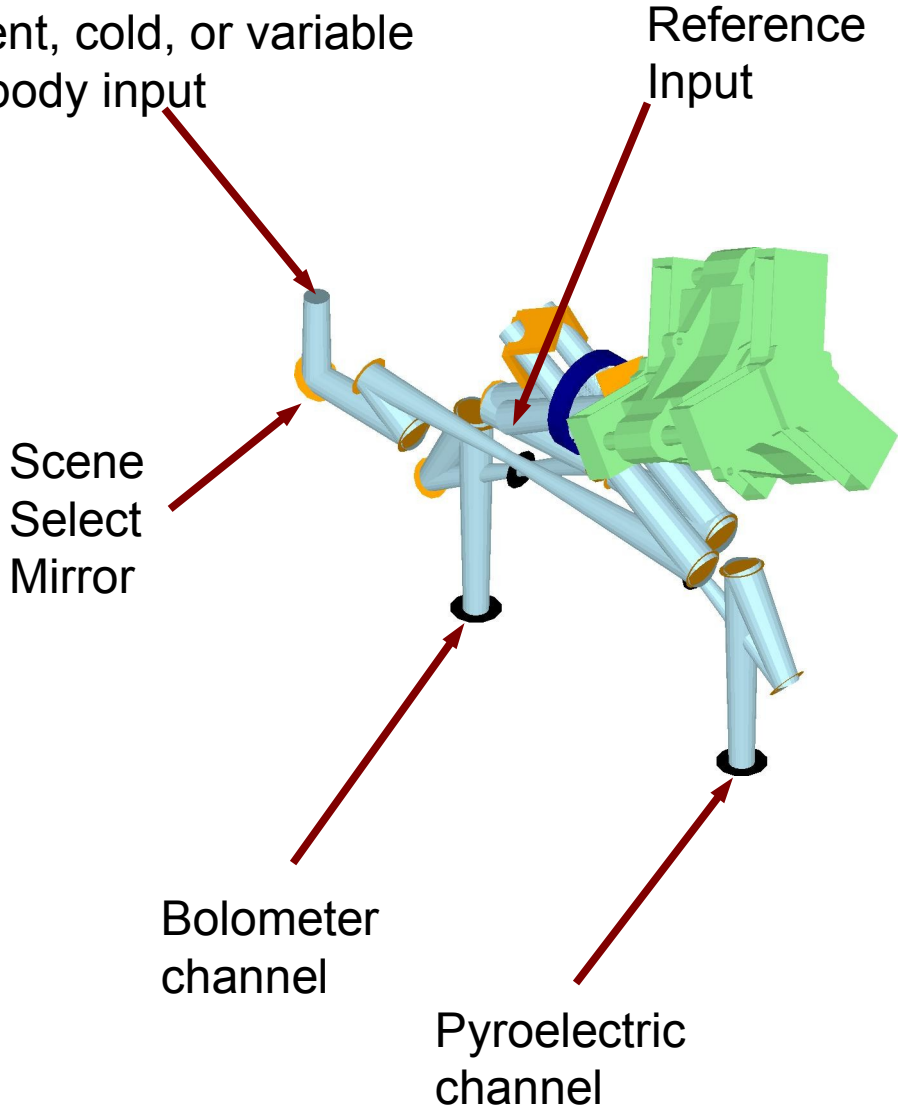

Langley Research Center

Infrared and Metrology Raytrace

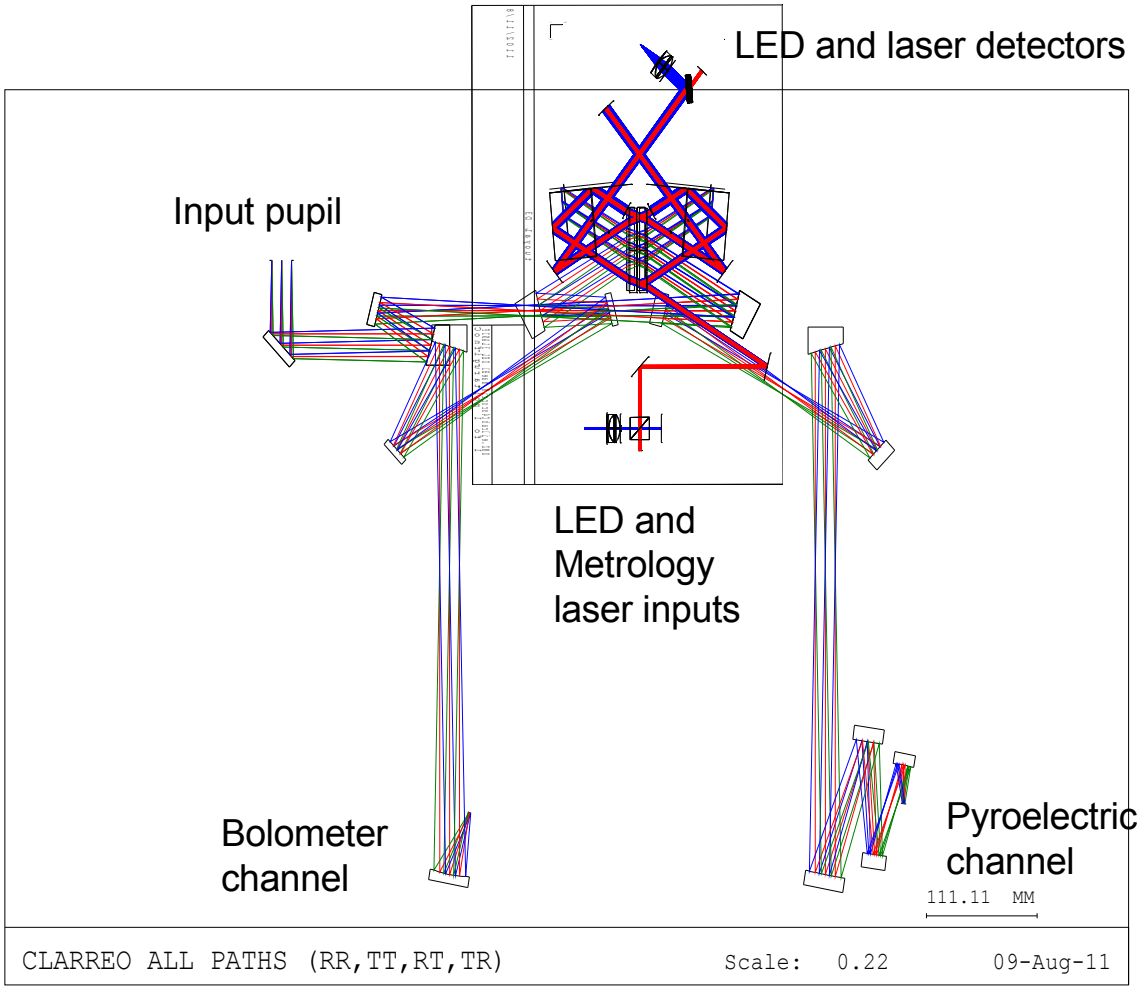

Infrared and Metrology Paths

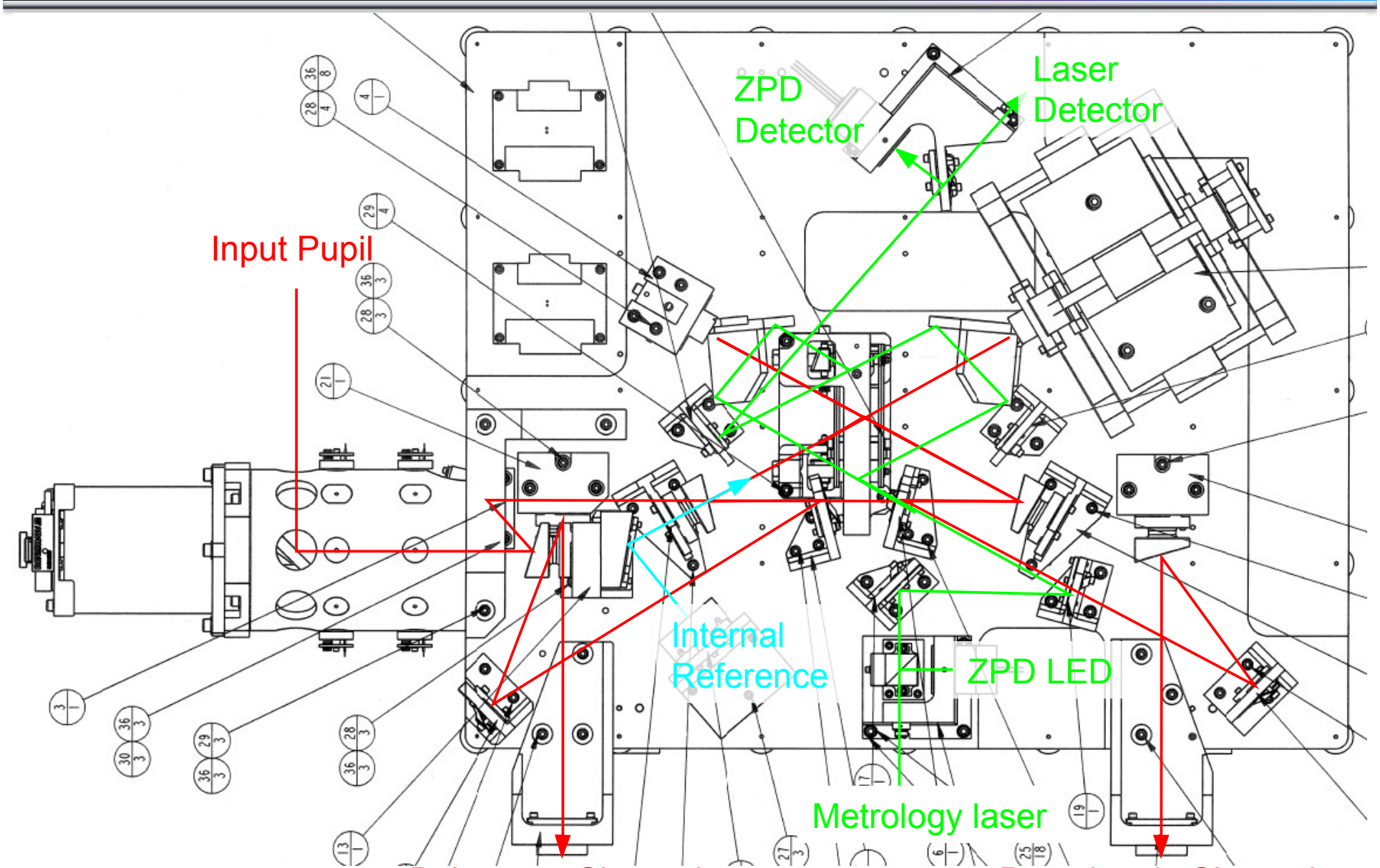

Infrared Ray trace

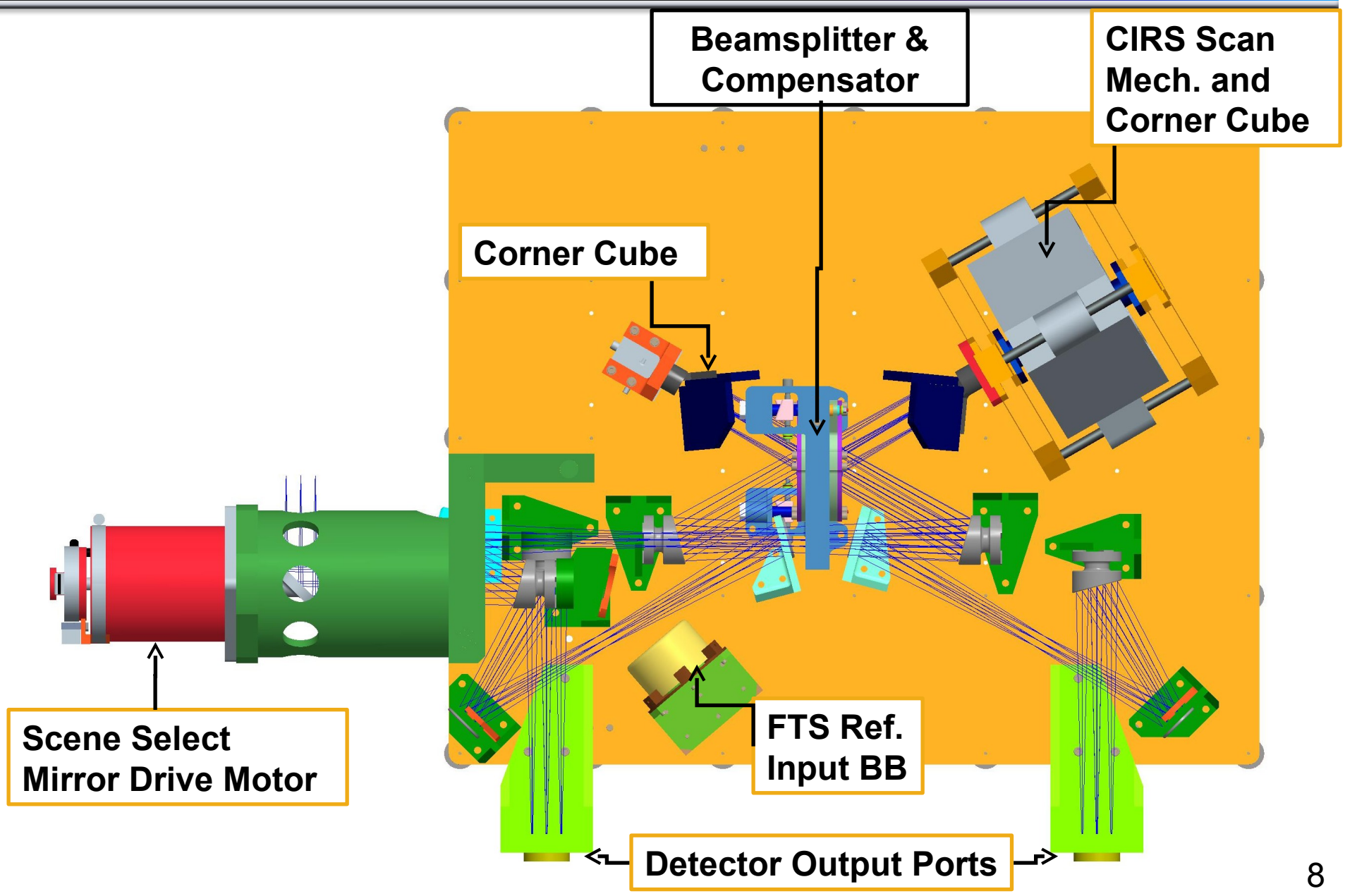

Optical Bench Temperature Uniformity

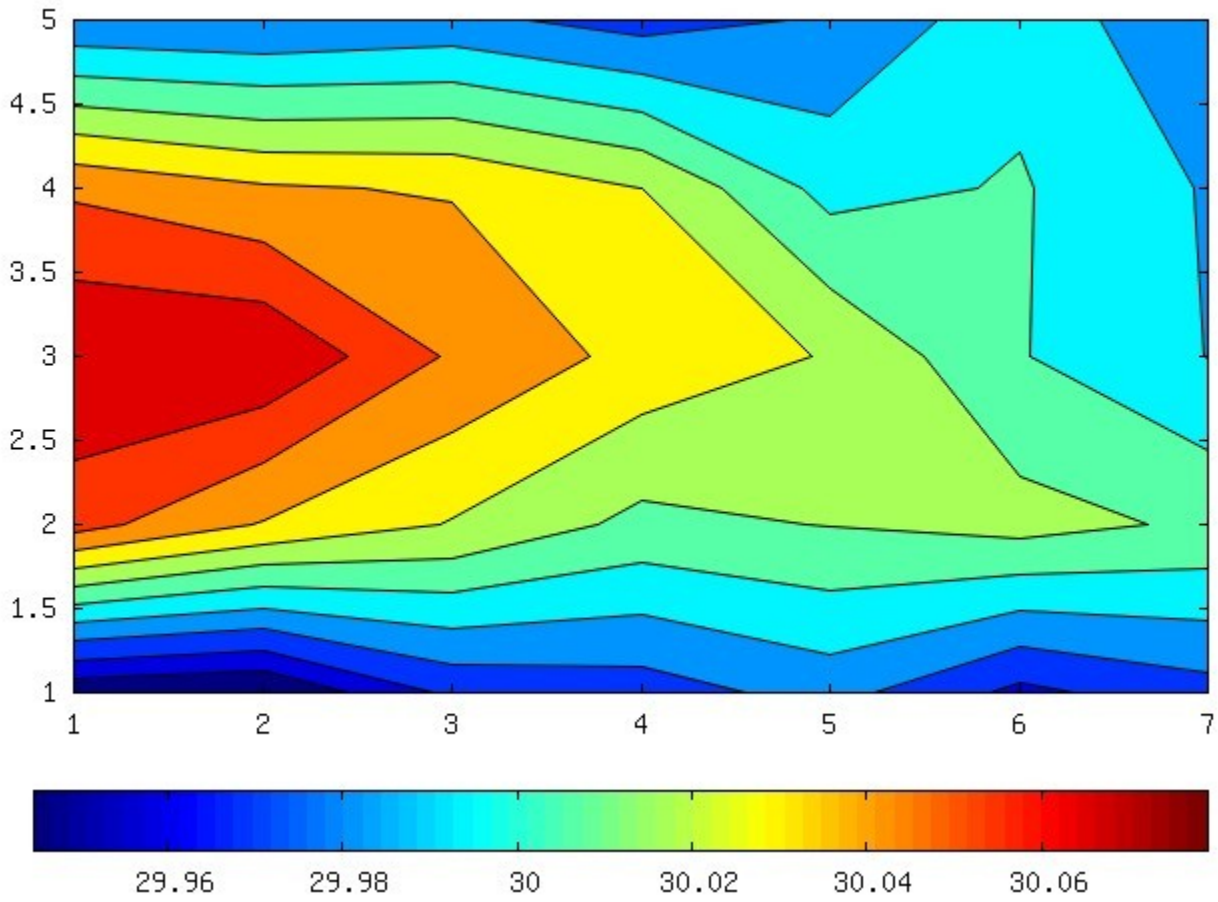

Optical Bench Temperature Stability

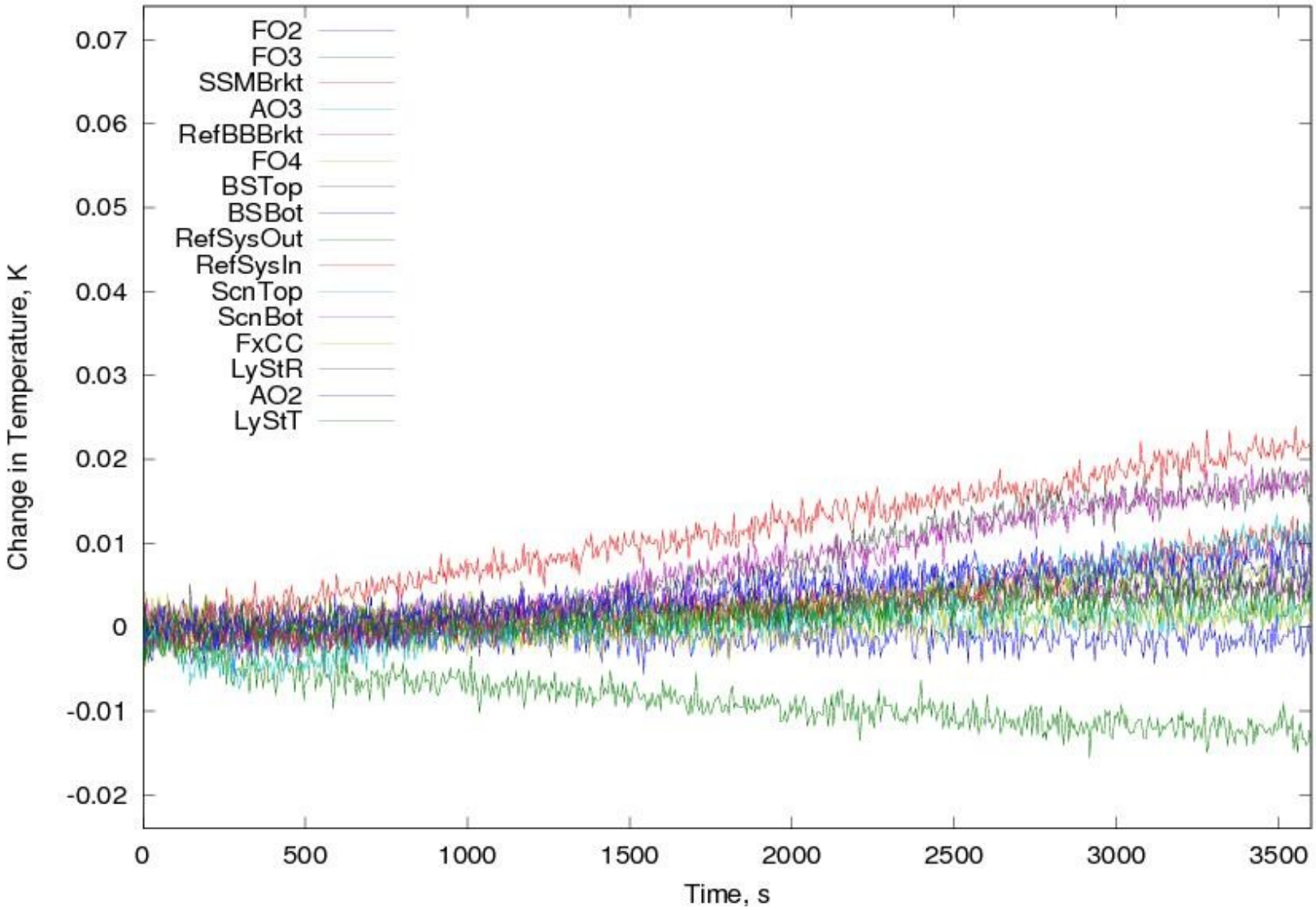

Observation Sequence

- Wait for VTBB temperature to stabilize (2-3 hours).
- Start observation sequence:
  - Position SSM at ABB during FTS flyback (1s);
  - Scan optical path difference (OPD) from +0.25 cm to -0.25 cm while observing ABB (2s);
  - Reposition SSM at CSS during FTS flyback (1s);
  - Scan OPD from +0.25 cm to -0.25 cm at CSS (2s);
  - Reposition SSM at VTBB during flyback (1s);
  - Scan OPD from +1 cm to -1 cm at VTBB (8s);
  - Complete cycle takes 15s; calibration spectra at ¼ resolution, VTBB spectra at full resolution.
- Repeat for ~2 hours (460 VTBB observations).
- Proceed to next VTBB plateau.

Interferogram Data

- After a programmable delay following each positive metrology laser fringe zero crossing, we:
  - Sample the bolometer channel output;
  - Sample the pyroelectric channel output;
  - Record the fringe crossing time for each sample.
- Every 200 samples we also sample detector DC levels and other FTS scan-related engineering data.
- A broadband LED and detector is used to provide a zero path difference (ZPD) reference location for each interferogram (IGM).

Interferogram preprocessing

- After extracting IGMs from raw data files and performing quality control checks:
  - Correct IGM baselines for transients related to changing scene temperature and electronic time constants;
  - Correct Pyroelectric data for velocity variations by scaling each sample by the ratio of the actual sample rate to the nominal sample rate: $I'(x) = I(x)\nu_{act}(x)/\nu_{nom}$;
  - Correct Bolometer data are corrected for responsivity variations proportional to temperature-related changes in bolometer resistance by scaling IGM by the ratio of the nominal detector DC voltage to the actual DC voltage: $I'(x) = I(x)V_{nom}/V_{act}(x)$.
- IGMs are centered using the ZPD data and truncated to the proper length:
  - ±2350 points for ABB, CSS;
  - ±9394 points for VTBB.

Transient Correction

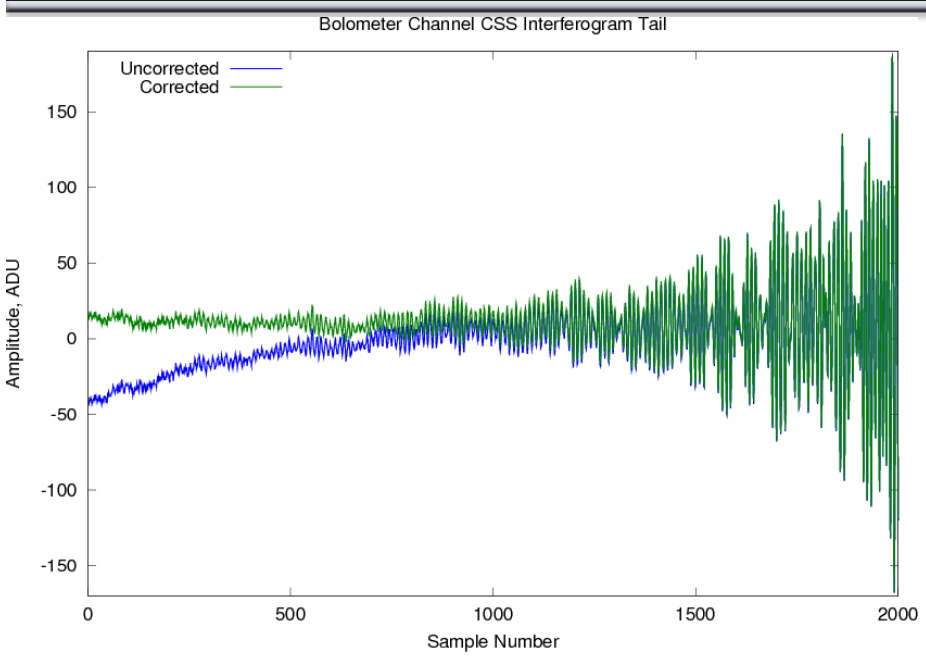

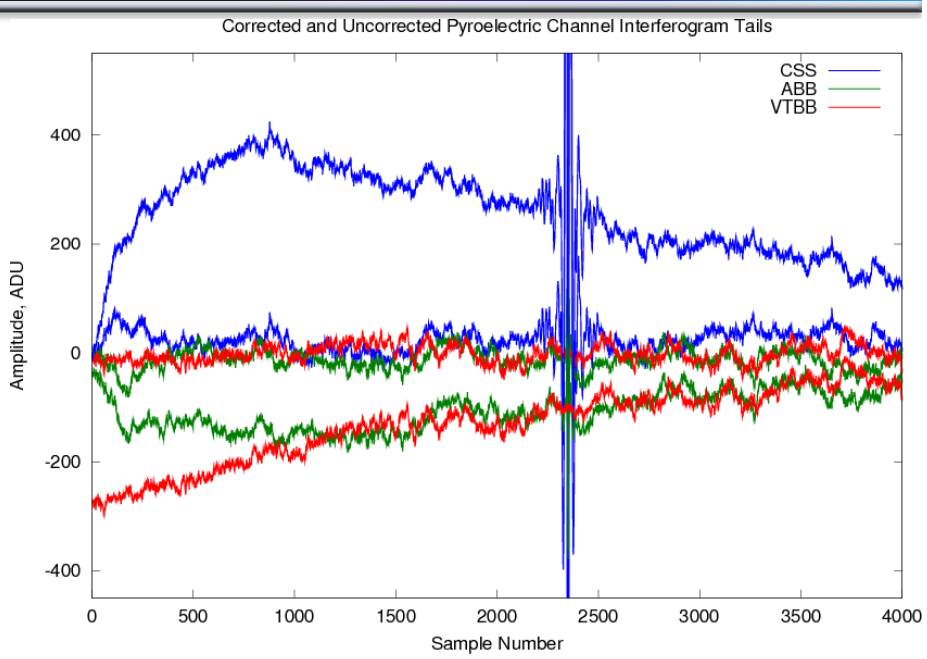

Bolometer transient modeled with a single time constant (0.18 s) from the preamp DC block filter:

$$V(t) = V_0(t) + V_T e^{-t/0.18}$$

Pyroelectric transient modeled with two time constants: one (0.18 s) from the preamp DC block filter, and another (1 s) from the detector electronic time constant:

$$V(t) = V_0(t) + V_{T1} e^{-t/0.18} + V_{T2} e^{-t}$$

Scan Velocity Variations

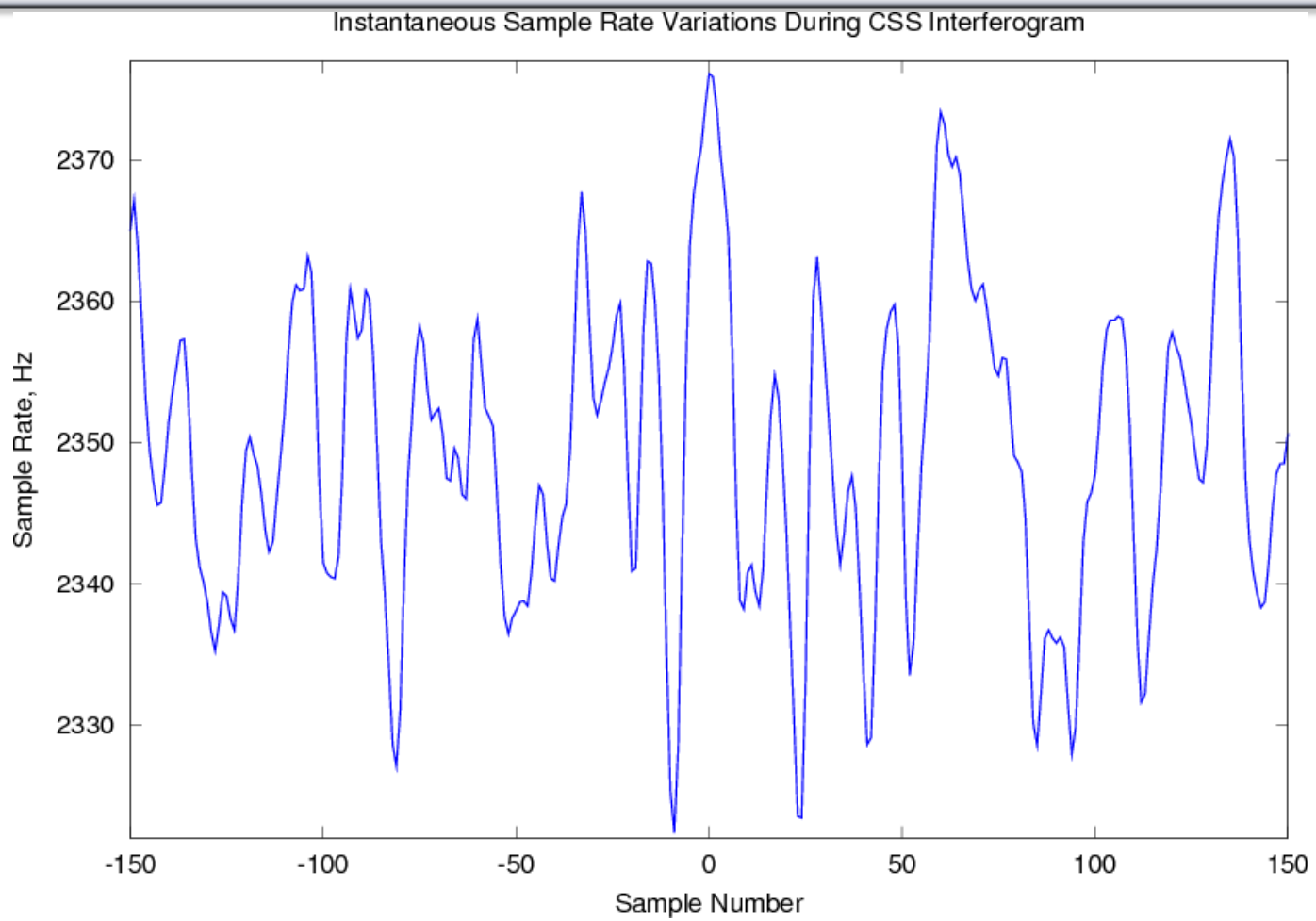

Due to the 1/f response of the pyroelectric detector, relative response is proportional to 1/(relative velocity). Because we record the time for individual samples, we can estimate the instantaneous velocity and correct for the effect of velocity variations.

Bolometer Channel DC IGMs

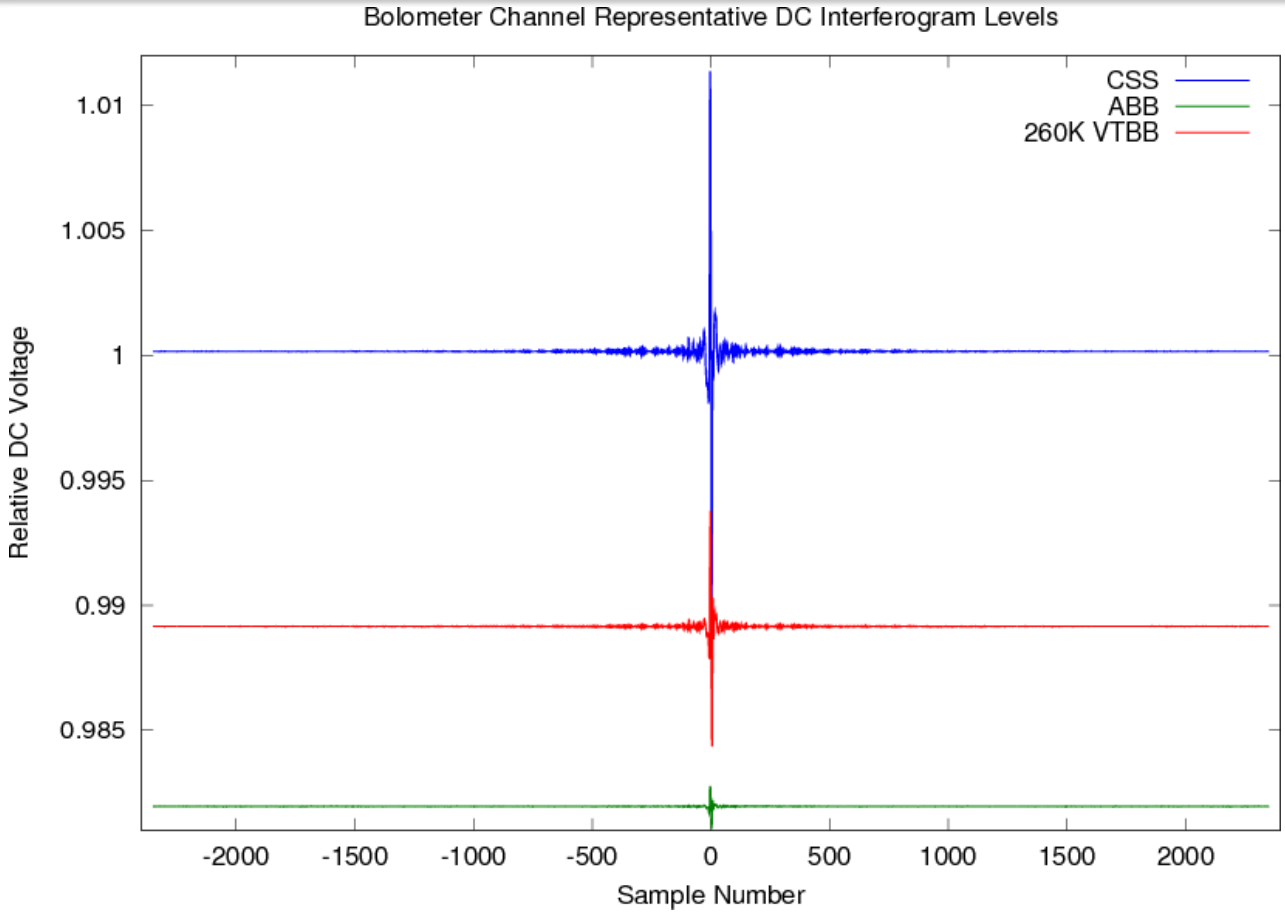

The bolometer is a thermal detector that responds to a change in radiative input by a change in temperature. The change in temperature causes a change in bolometer resistance that is in turn proportional to resistance, resulting in nonlinear response that can be corrected by normalizing by the instantaneous resistance (or relative DC voltage as shown above).

Calibration Process

- After preprocessing:
  - Linear fit of CSS IGMs within 130s of VTBB IGM to estimate average at time of VTBB observation;
  - Use CSS radiance model to estimate L_{CSS} at time of VTBB observation;
  - Linear fit of ABB IGMs within 130s of VTBB IGM to estimate average at time of VTBB observation;
  - Use ABB radiance model to estimate L_{ABB} at time of VTBB observation;
  - Use VTBB radiance model to estimate L_{VTBB} for later comparison with calibrated spectrum L'_{VTBB};
  - Zero-pad ABB and CSS IGMs to length of VTBB IGM;
  - Calculate Fourier transforms (FT) and calibrate:

$$L'_{VTBB} = L_{CSS} + (L_{ABB} - L_{CSS}) * \frac{FT(I_{VTBB} - I_{CSS})}{FT(I_{ABB} - I_{CSS})}.$$

Interferogram Repeatability

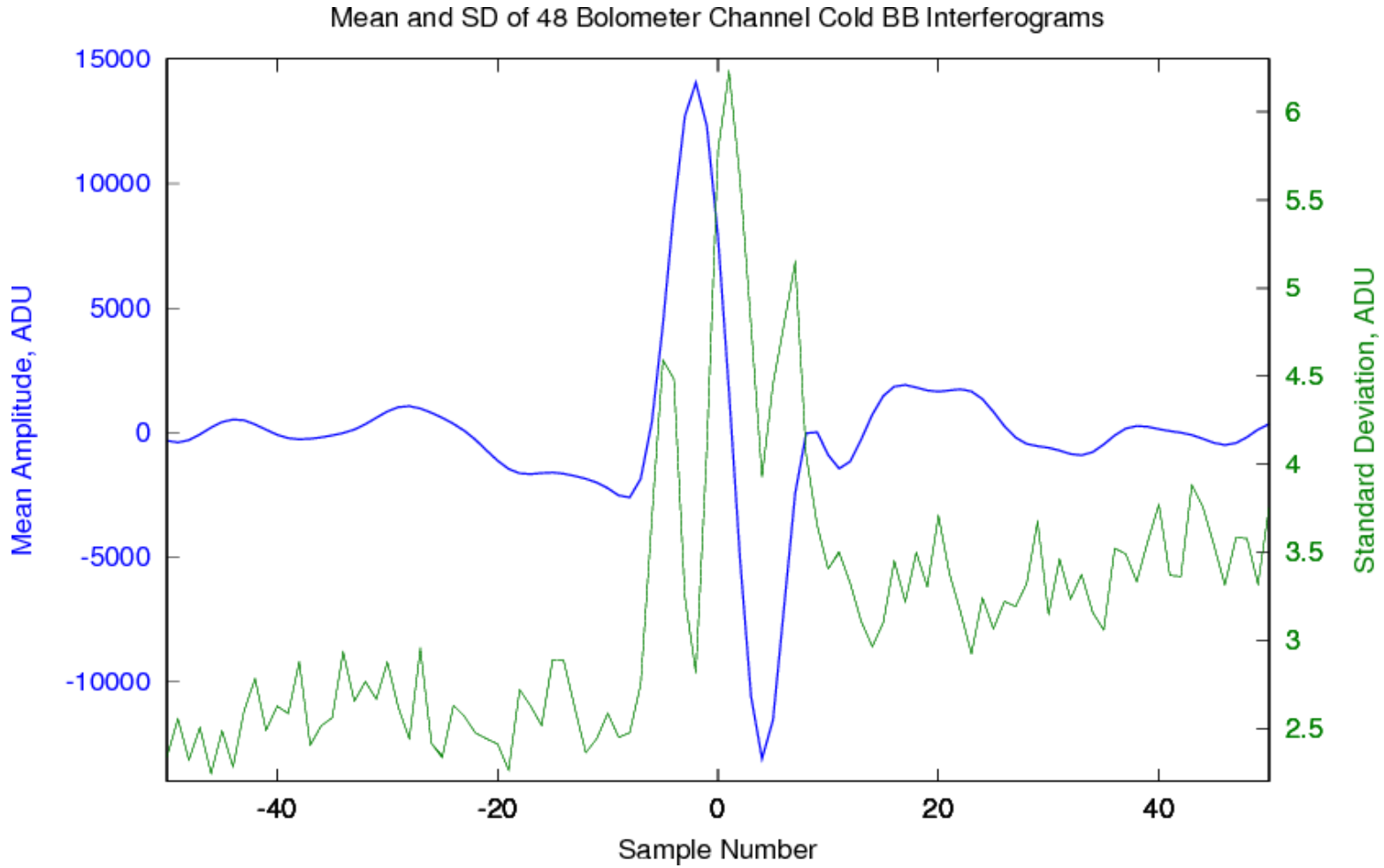

• Excess noise in ZPD region caused by small random sample position error, roughly 2x the noise floor.

ABB Radiance Model

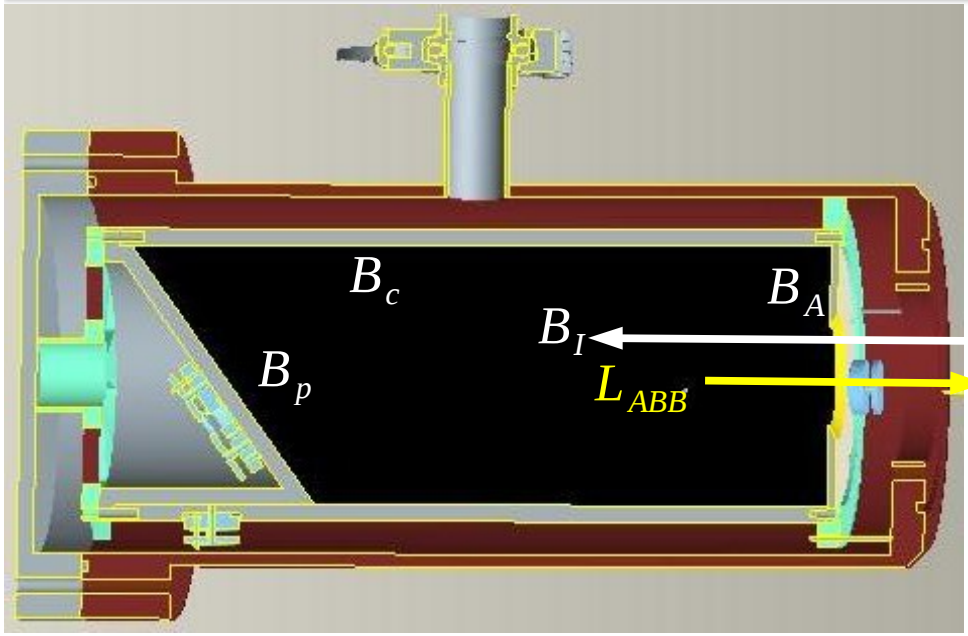

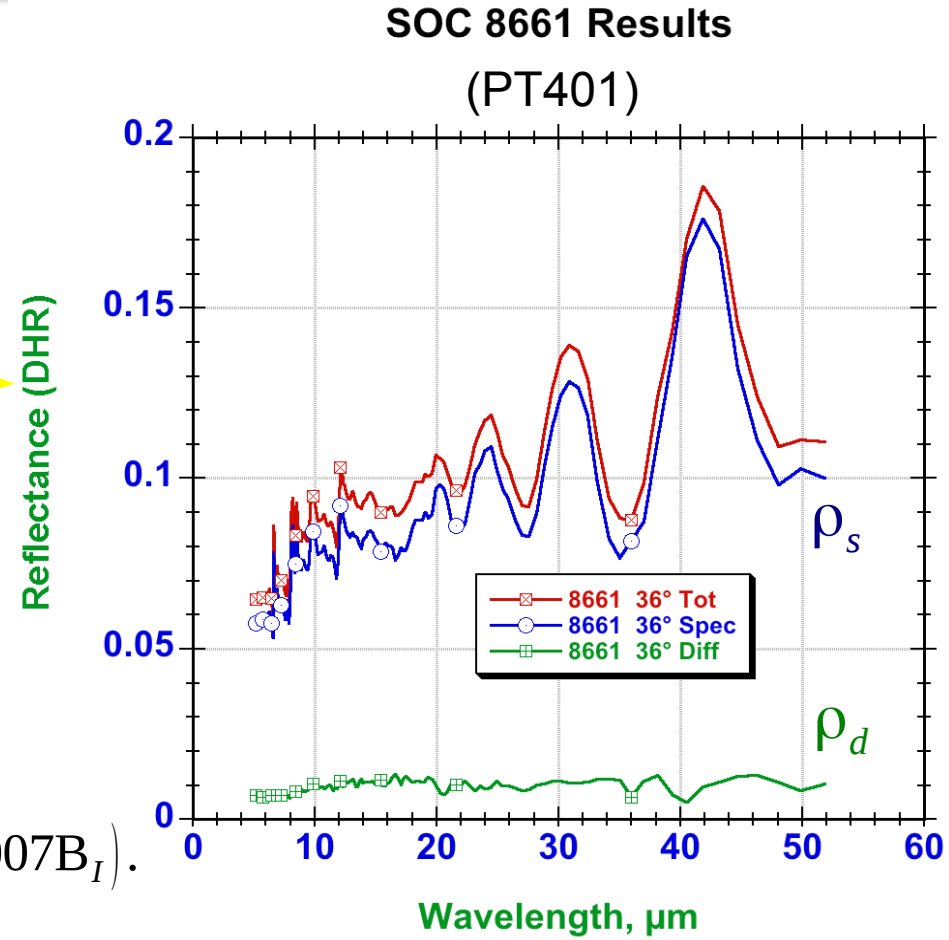

$$B_s \equiv \frac{B_p + \rho_s B_c}{(1+\rho_s)};$$

$$L_{ABB} = (1-\rho_d) B_s + \rho_d \left(0.954 B_c + 0.039 B_A + 0.007 B_I\right).$$

$$B_x \equiv \frac{\alpha \bar{\nu}^3}{\left(e^{\beta \bar{\nu}/T_x} - 1\right)}; \alpha \equiv 2hc^2; \beta \equiv hc/k.$$

Comparison with Virial INCA333

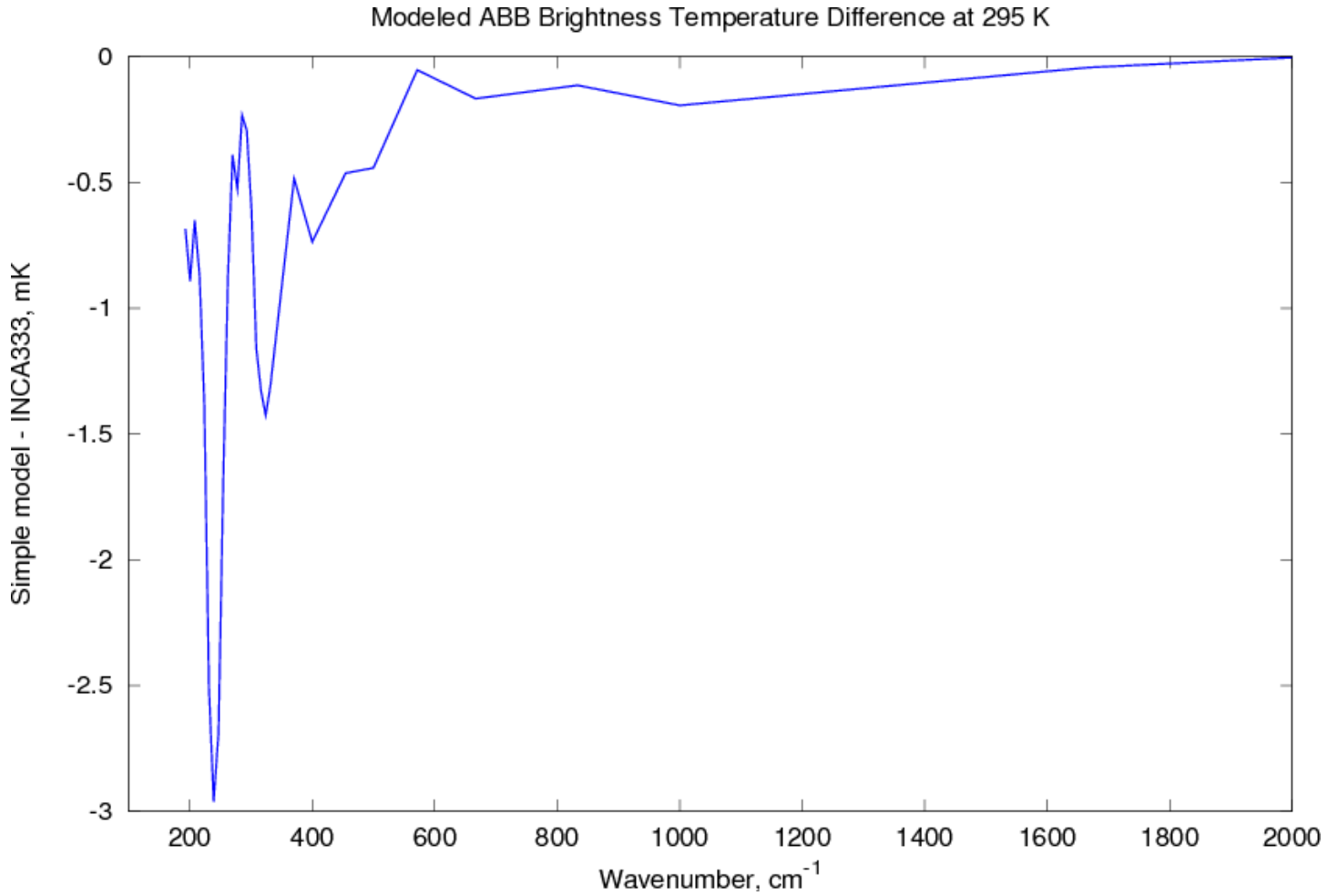

Brightness temperature differences are not significant.

CSS Radiance Model

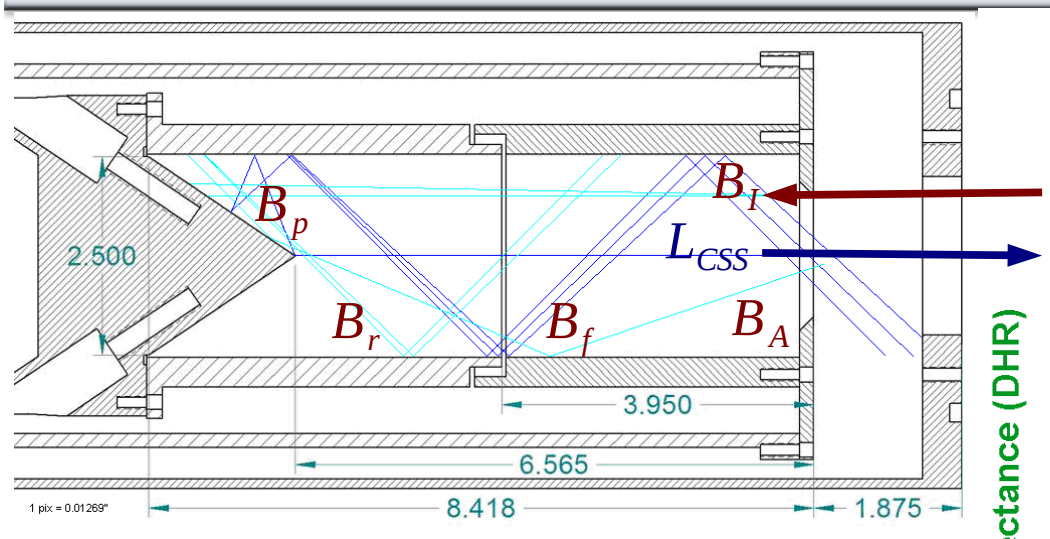

$$B_s \equiv \frac{B_p + \rho_s B_r}{(1+\rho_s)};$$

$$L_{CSS} = (1-\rho_d) B_s + \rho_d \left(0.892 B_r + 0.083 B_f + 0.013 B_A + 0.012 B_I\right).$$

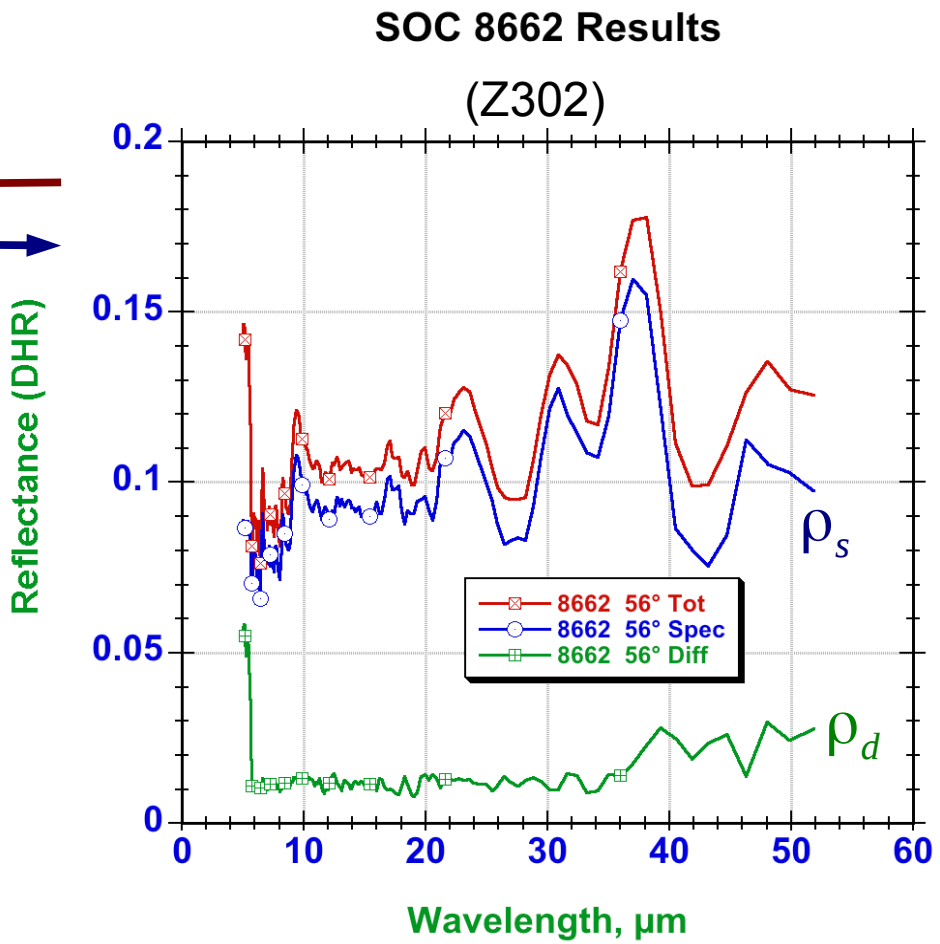

$$B_x \equiv \frac{\alpha \bar{\nu}^3}{\left(e^{\beta \bar{\nu}/T_x} - 1\right)}; \alpha \equiv 2hc^2; \beta \equiv hc/k.$$

Comparison with Virial STEEP3

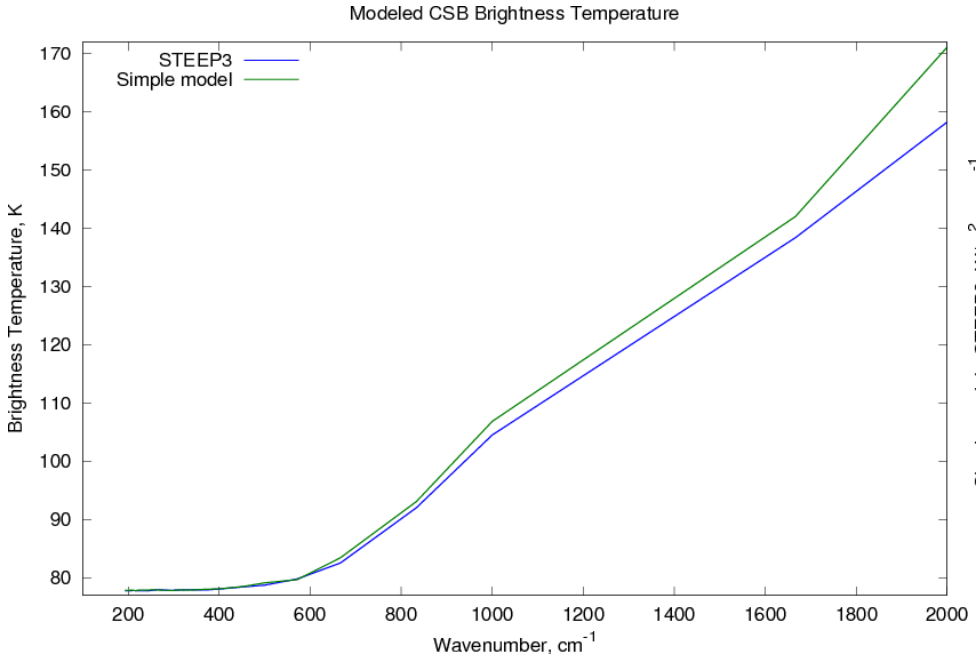

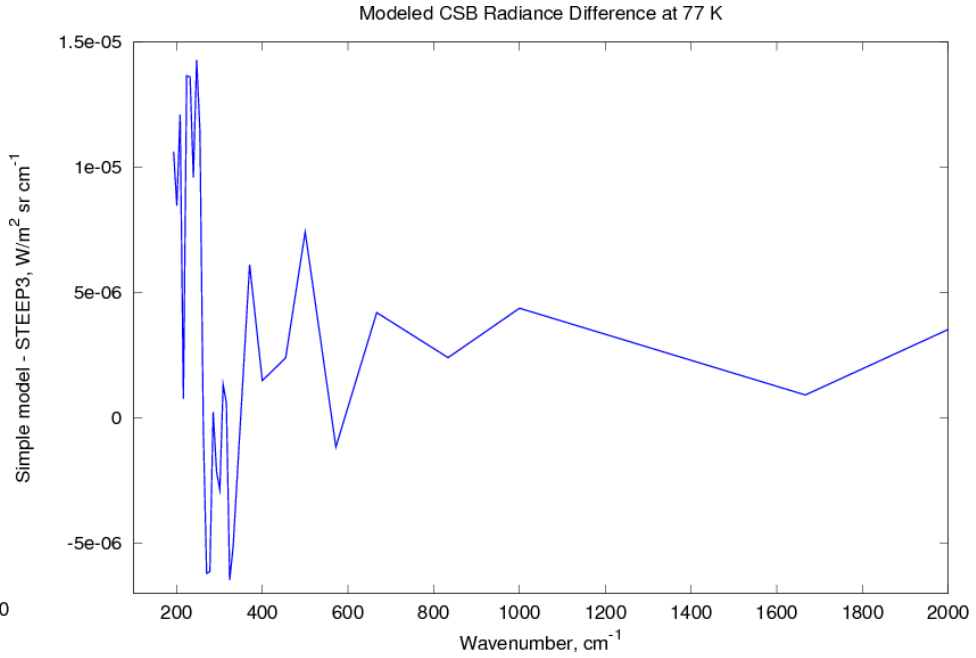

Although brightness temperature differences are large at high wavenumber, the radiance difference is insignificant.

VTBB Radiance Model

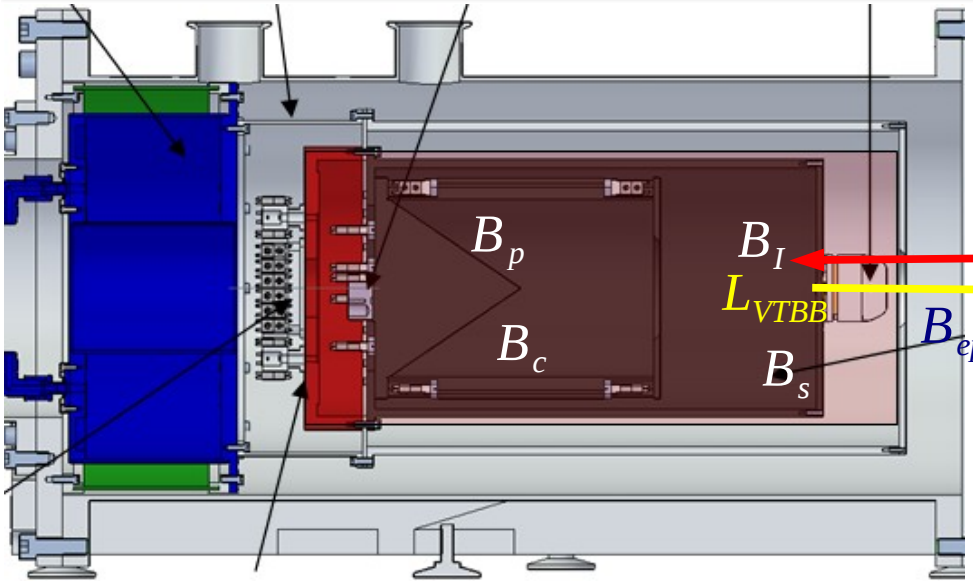

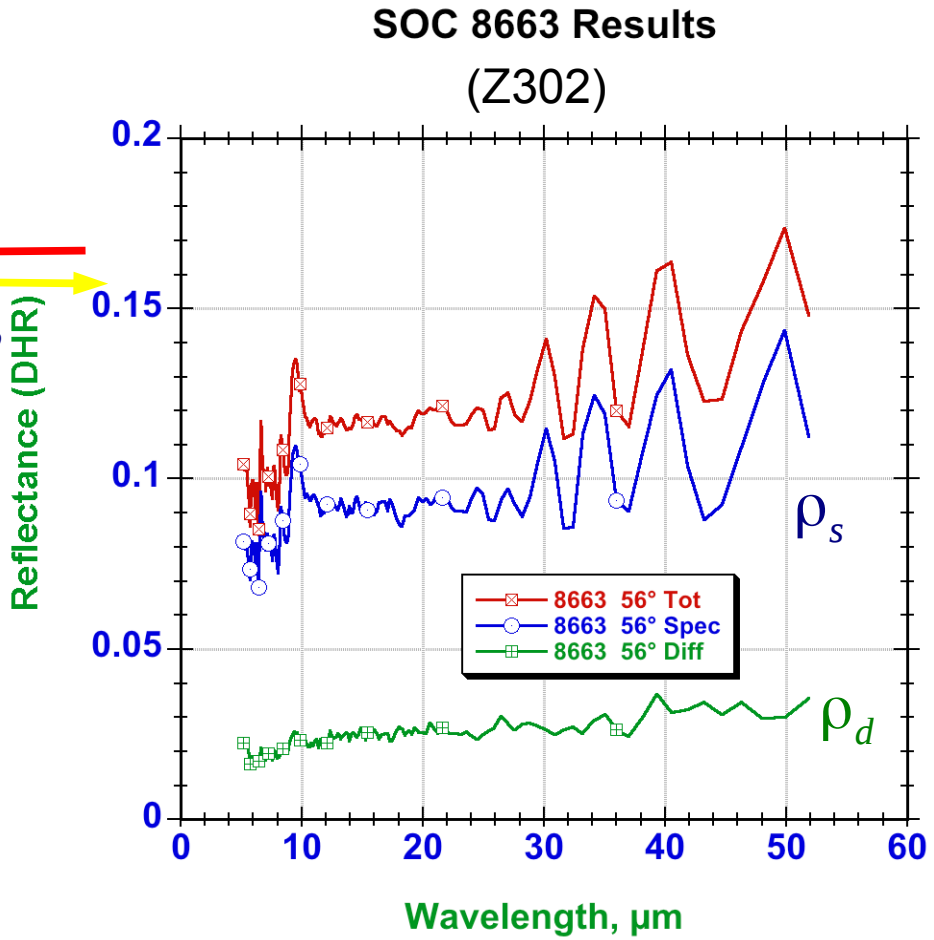

$$B_s \equiv \frac{B_p + \rho_s B_c}{(1+\rho_s)};$$

$$L_{VTBB} = (1-\rho_d) B_s + \rho_d (0.965 B_c + 0.027 B_s + 0.004 B_{ep} + 0.004 B_I).$$

$$B_x \equiv \frac{\alpha \bar{\nu}^3}{\left(e^{\beta \bar{\nu}/T_x} - 1\right)}; \alpha \equiv 2hc^2; \beta \equiv hc/k.$$

Comparison with Virial STEEP3

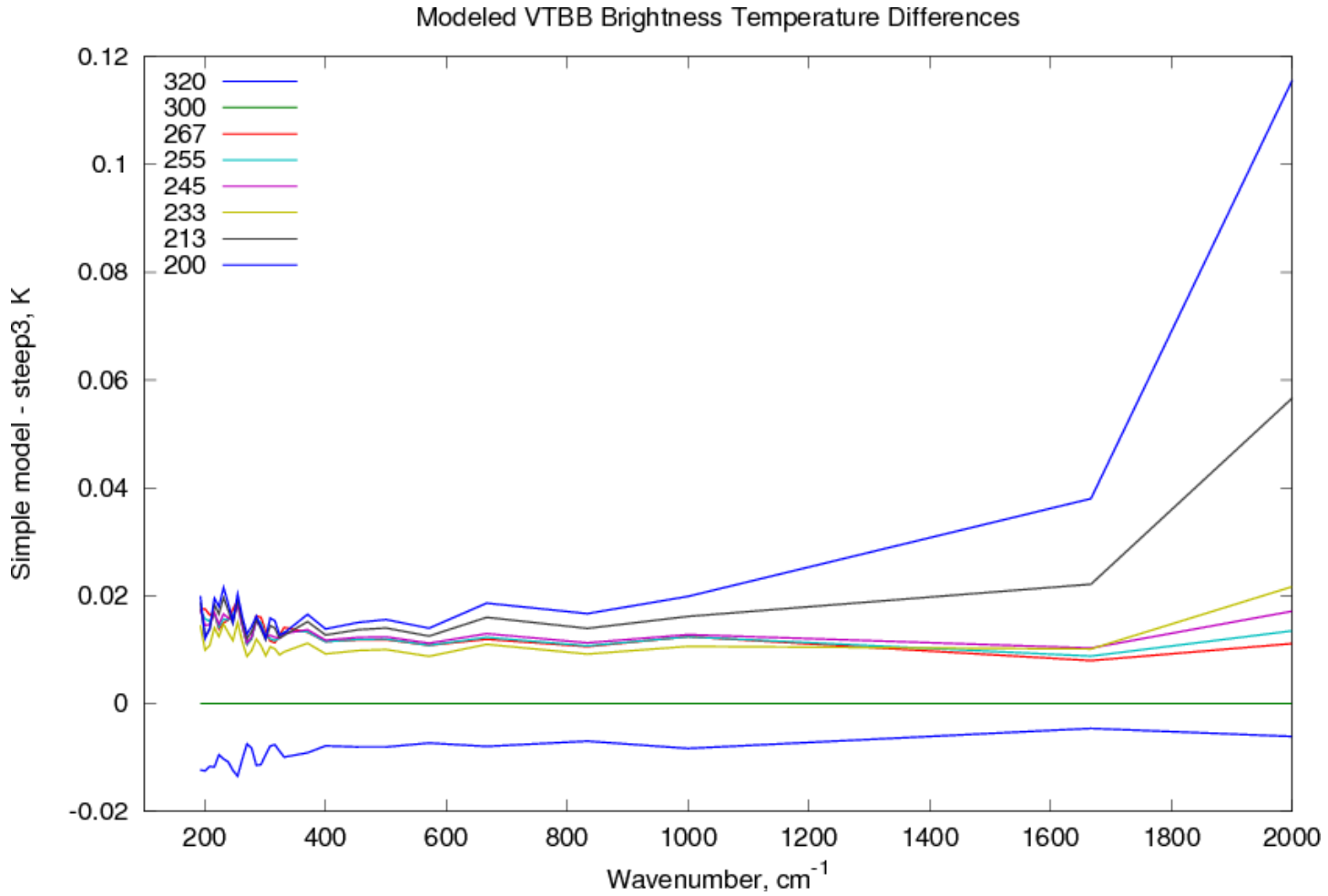

Preliminary results calculated from temperatures measured during cooldown, resulting in large gradients. Some of the discrepancy results from different interpretations of the surface temperature distribution implied by the temperature measurements. Calculations will be repeated with equilibrium temperature values.

CHILR Cavity Reflectance Measurements

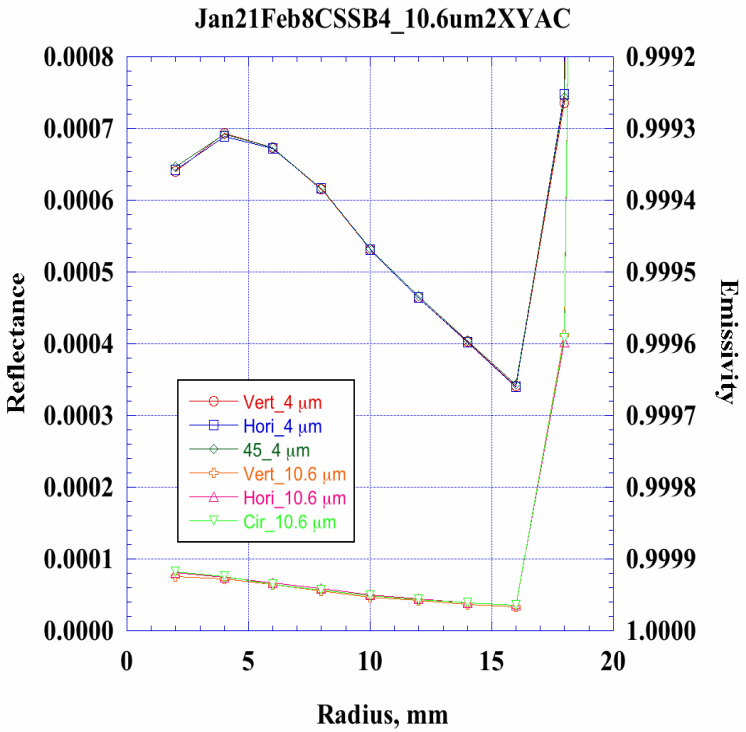

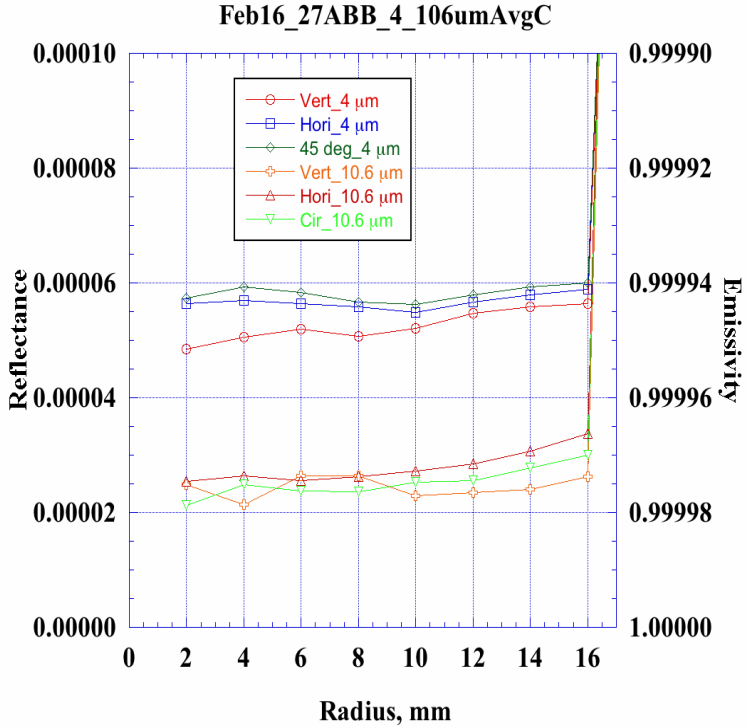

CHILR 10.6 µm CSS reflectance: 0.5×10^{-4}

Model: $1.6 \pm 1.0 \times 10^{-4}$

CHILR 4 µm CSS reflectance: 5.5×10^{-4}

Model (5 µm): $6.6 \pm 1.0 \times 10^{-4}$

CHILR 10.6 µm ABB reflectance: 2.5×10^{-5}

Model: $6.7 \pm 5.6 \times 10^{-5}$

CHILR 4 µm ABB reflectance: 5.5×10^{-5}

Model (5 µm): $4.6 \pm 5.6 \times 10^{-5}$

Estimated uncertainty of 0.008 in SOC diffuse reflectance measurements

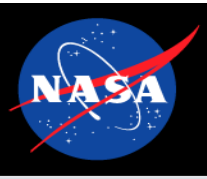

Langley Research Center

ABB Thermistor Accuracy (295 K)

Source	Standard Uncertainty (u_j)	Reference
ITS90 TP (H_2O) (Type A)	0.03 mK	NIST IR5319
SPRT Calibration (k=1)	0.25 mK	Hart Scientific calibration report
Superthermometer SPRT ratio (k=1)	0.08 mK	Hart Scientific technical guide (1594A)
SPRT drift (type B, rect)	0.29 mK	Checked with LaRC TPW cell
Cal bath gradients (type B, rect)	1.15 mK	LaRC estimate from hysteresis
Superthermometer thermistor ratio (k=1)	0.008 mK	Hart Scientific technical guide (1594A)
Thermistor repeatability (type B, rect)	1.04 mK	Estimate from LaRC experience
Steinhart-Hart fit error (type B, rect)	0.4 mK	Estimate from fit residuals
Total Calibration:	**1.65 mK**	
Blackstack accuracy (type B, rect)	4.2 mK	5K thermistor at 295K; Hart Scientific 1560 + 2564 literature
Total	**4.5 mK, k=1 (9 mK, k=2)**	

CSS PRT Accuracy (77 K)

Source	Standard Uncertainty (u_j)	Reference
ITS90 TP (Ar) (Type A)	0.05 mK	NIST IR5319
PRT repeatability (Type B, rect)	2.9 mK	Lake Shore PT 103 literature
PRT calibration (k=1)	5.6 mK	Lake Shore PT 103 literature
Mounting change correction uncertainty (type B, rect)	0.4 mK	Space Dynamics Lab estimate
Drift (type B, rect)	0.6 mK	Space Dynamics Lab estimate
Hysteresis (type B, rect)	1.7 mK	Space Dynamics Lab estimate
Total Calibration (77 K)	**6.6 mK**	
Blackstack accuracy (type B, rect)	1.4 mK	Hart Scientific literature, 1560 + 2562 PRT module
Self heating uncertainty (type B, rect)	6 mK	Space Dynamics Lab estimate
Blackbody gradients (type B, rect)	12 mK	Space Dynamics Lab worst case model estimate
Total	**15 mK, k=1 (30 mK, k=2)**	

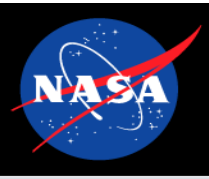

Langley Research Center

VTBB Thermistor Accuracy

Source	Standard Uncertainty, u_j			Reference
	200 K	260 K	320 K	
SPRT Calibration (k=1)	2.5 mK	2.5 mK	2.5 mK	Space Dynamics Lab test report
Blackstack SPRT readout accuracy (type B, rect)	3.9 mK	5.3 mK	6.7 mK	Hart Scientific literature
Blackstack thermistor readout accuracy (type B, rect)	1.9 mK	1.1 mK	2.9 mK	Hart Scientific literature (results for 2.5 kΩ thermistor)
SPRT drift (type B, rect)	1.2 mK	1.2 mK	1.2 mK	Space Dynamics Lab estimate
Cal bath gradients (type B, rect)	1.2 mK	1.2 mK	1.2 mK	LaRC estimate from ABB cal
Repeatability (type B, rect)	1.0 mK	1.0 mK	1.0 mK	LaRC estimate from ABB cal
Steinhart-Hart fit error (type B, rect)	0.4 mK	0.4 mK	0.4 mK	LaRC estimate from ABB cal
Total Calibration :	**5.4 mK**	**6.3 mK**	**8.0 mK**	
Blackbody gradients (type B, rect)	4.9 mK	4.9 mK	4.9 mK	Space Dynamics Lab model estimate
Blackstack thermistor readout (type B, rect)	1.9 mK	1.1 mK	2.9 mK	Hart Scientific literature; self heating included in original calibration
Total, k=1	7.6 mK	8.1 mK	9.8 mK	
Total, k=2	**15 mK**	**16 mK**	**20 mK**	

Blackbody Gradients and Drift

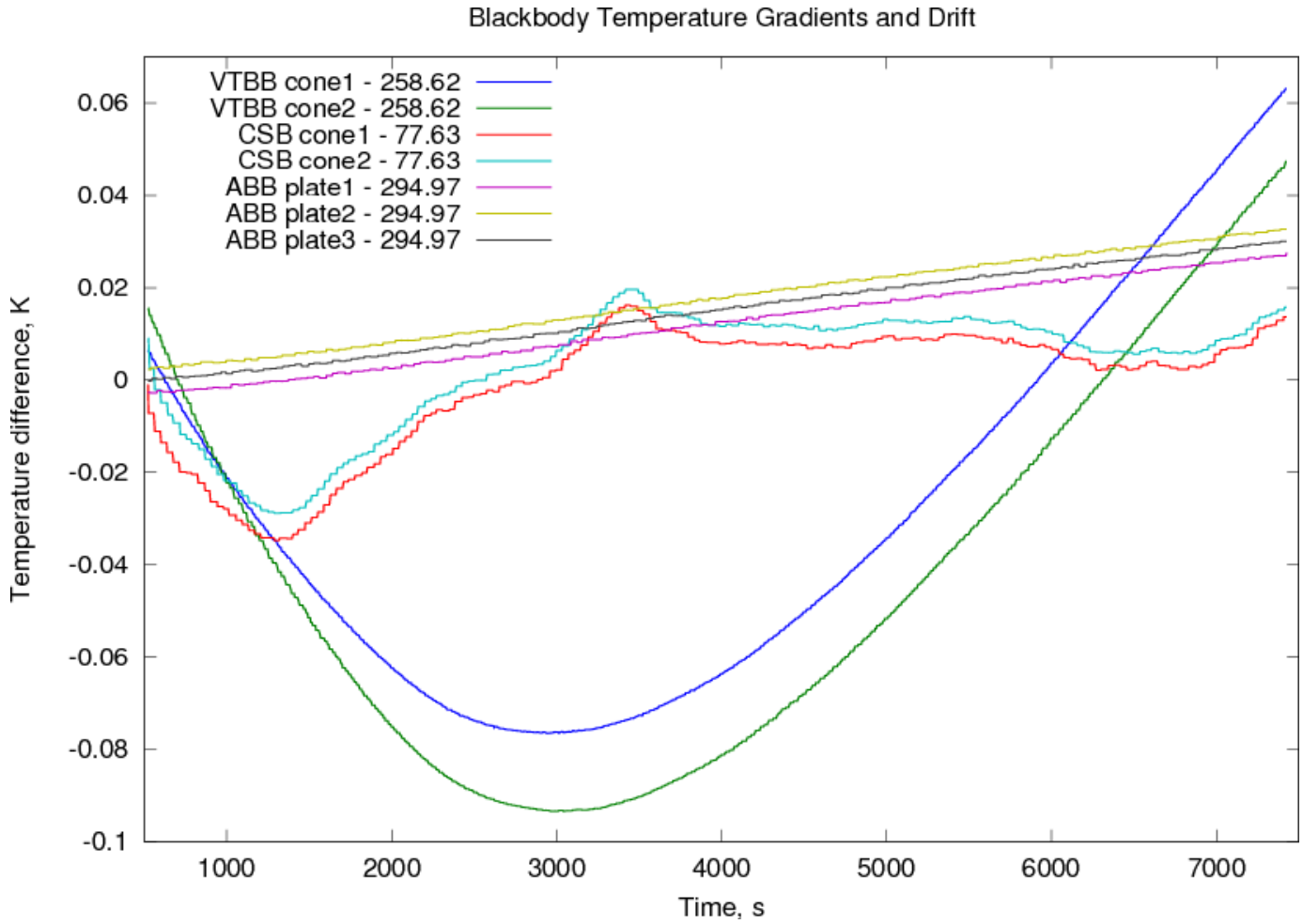

Bolometer and Pyro Responsivity

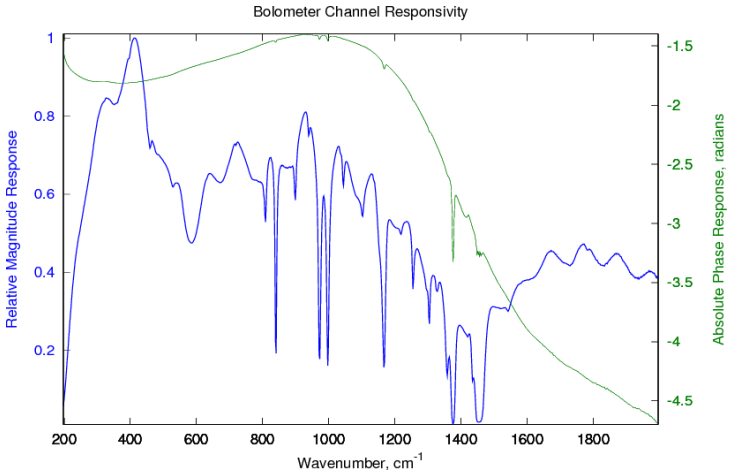

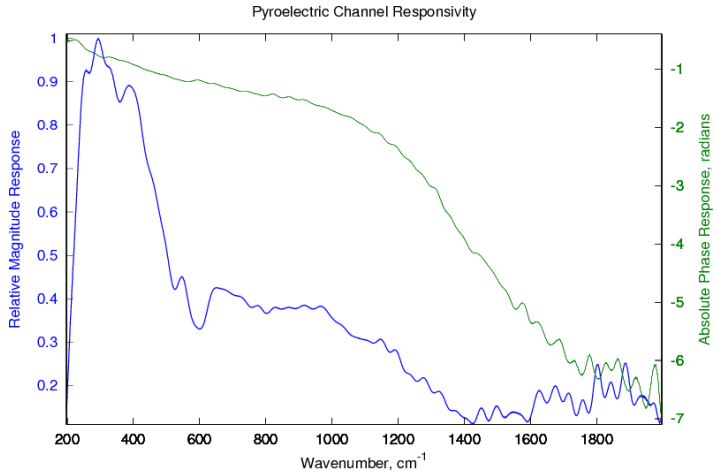

- Accuracy is affected by low or rapidly changing responsivity.
- Bolometer channel responsivity shows strong absorption features from polypropylene detector dewar window.
- Pyroelectric channel shows steep rolloff due to electronic frequency response, and absorption from 1400-1600 cm^{-1} from protective parylene coating on CsI detector window.

Calibrated Radiance

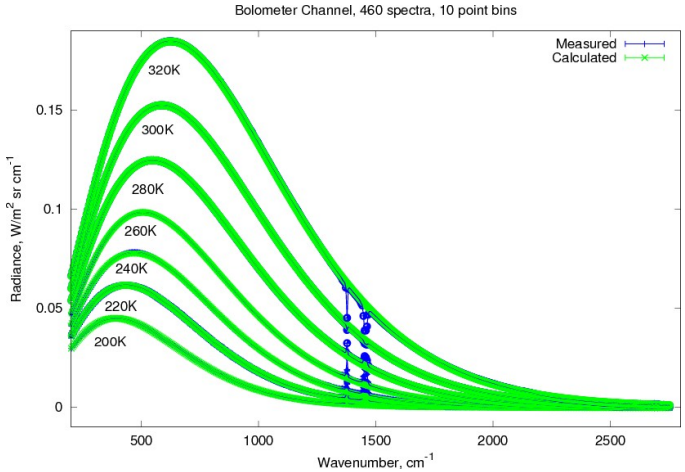

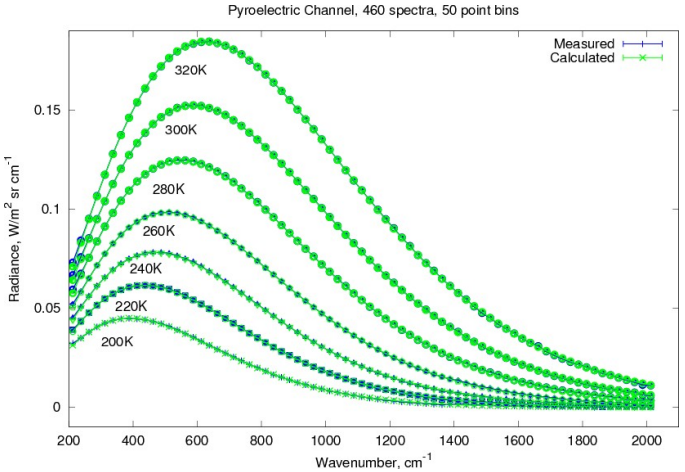

- Acquired roughly 2 hours of data at each dwell temperature
  - 460 variable temperature blackbody spectra at 0.5 cm^{-1} resolution.
  - 460 cold and ambient calibration blackbody views at 2 cm^{-1} resolution.
- Also binned spectrally: 10 points (5 cm^{-1}) for bolometer, 50 points (25 cm^{-1}) for pyroelectric.
- Standard errors (k=1) shown.

Brightness Temperature

- Expect best bolometer results below 1350 cm-1 due to window absorption
- Expect best pyro results below 1350 cm-1 due to detector window coating absorption and high frequency rolloff.
- Calculation includes scattering; note curvature at 200K

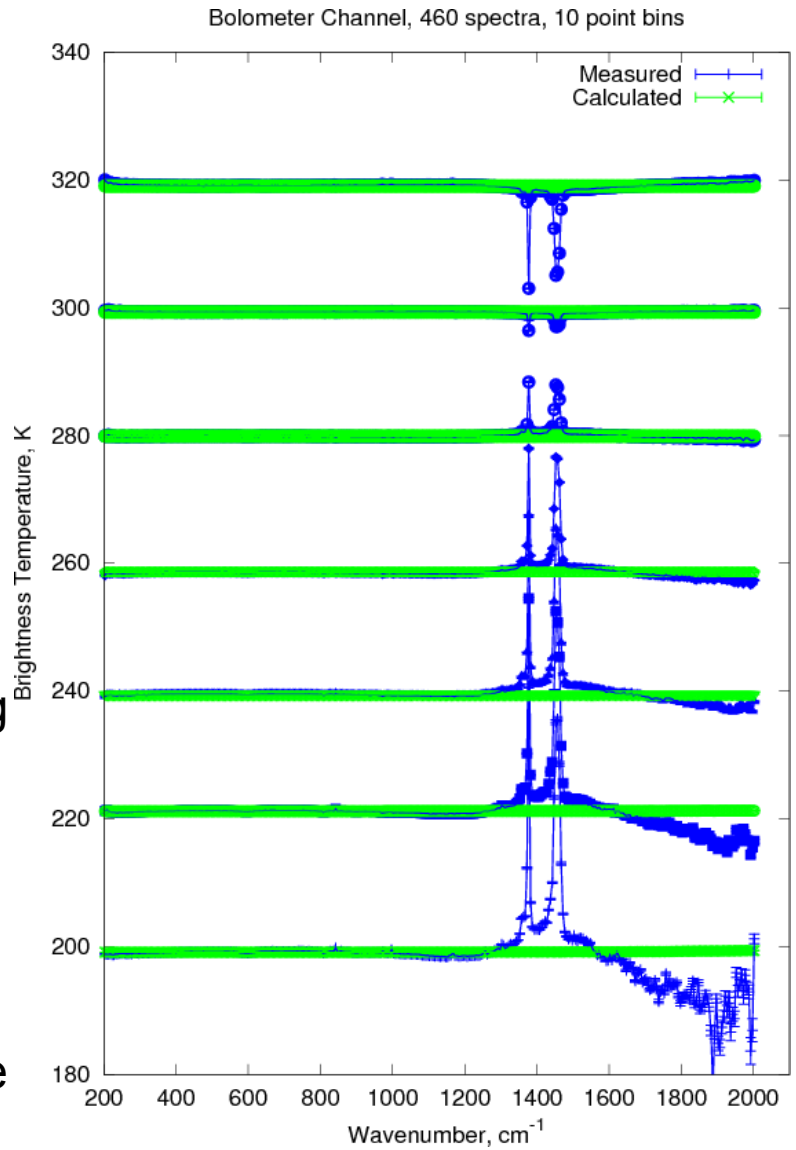

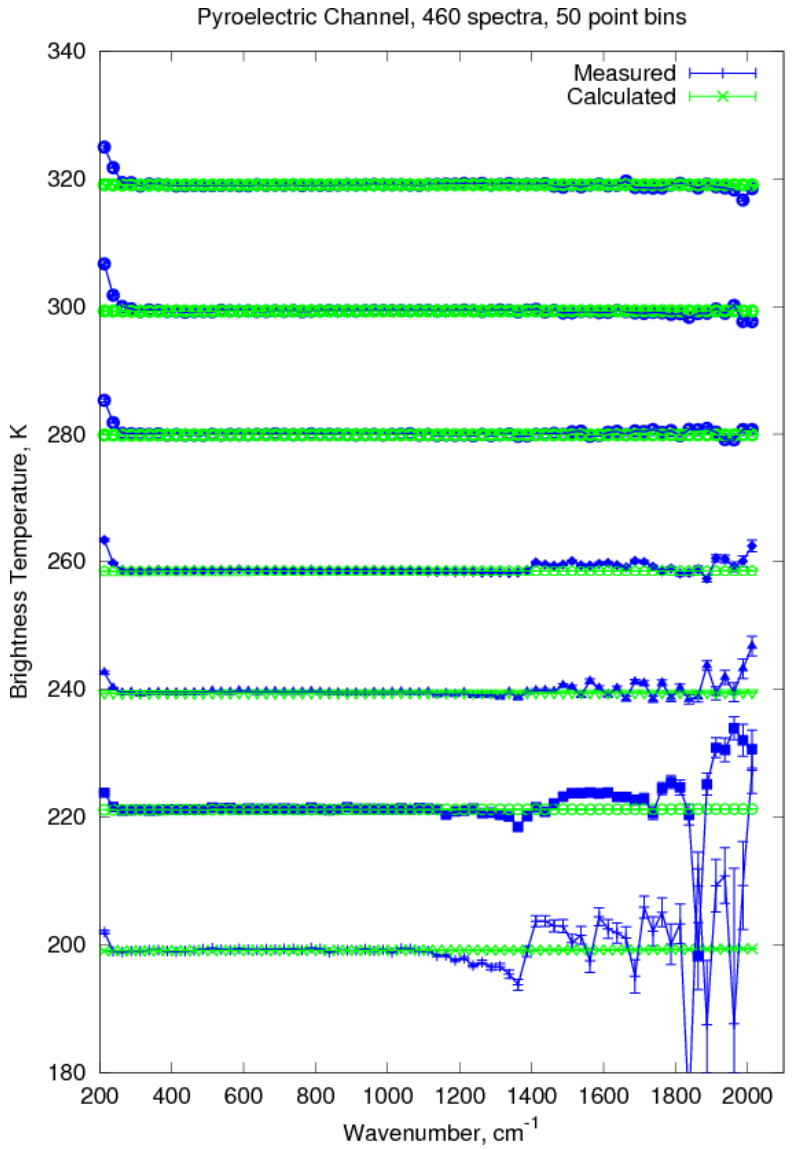

Radiance Difference

- Scale expanded 40x relative to previous calibrated radiance plot.
- Green line is origin for each offset plot.
- Systematic bolometer error and variation with temperature suggests uncorrected nonlinear behavior.

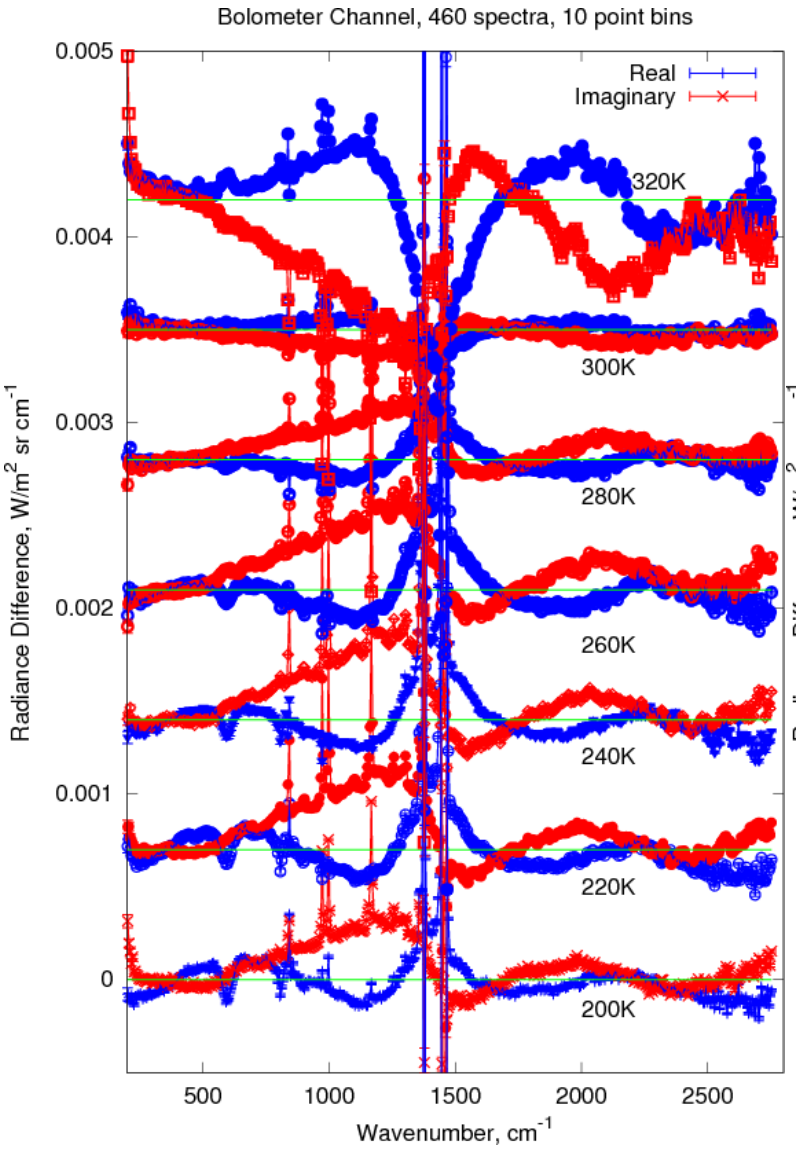

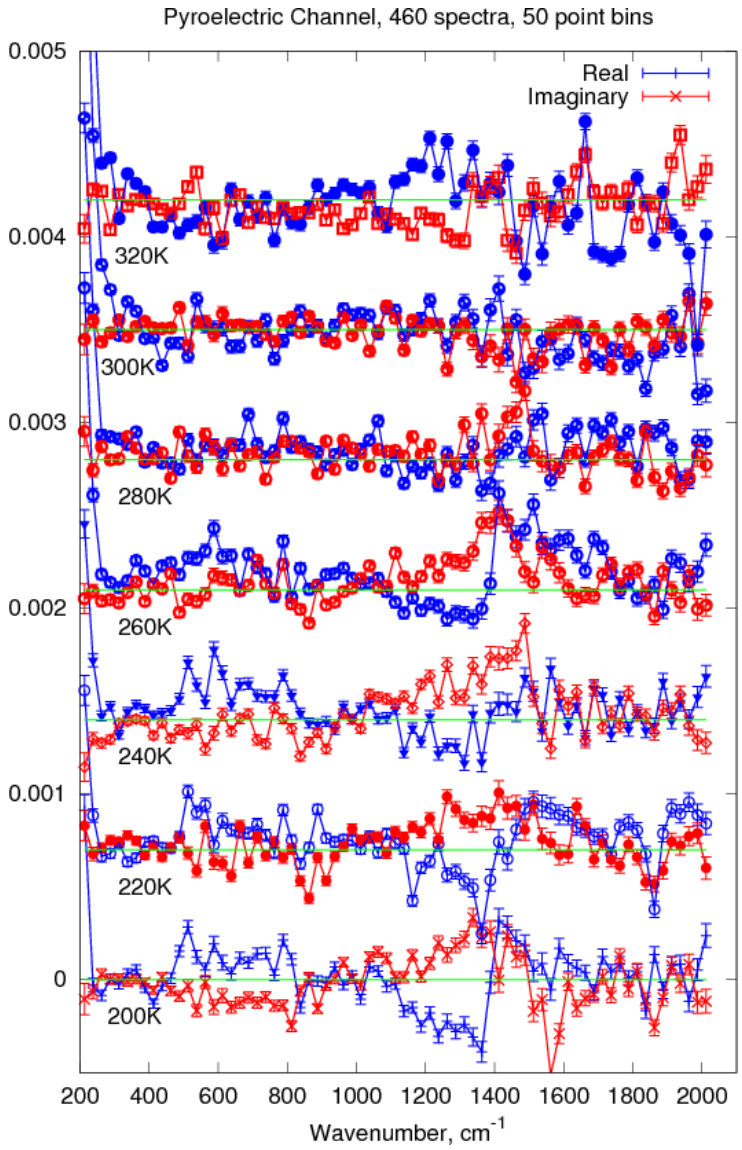

Temperature Difference

- Red line is origin for each offset plot; green lines indicate ±0.1K.
- k=1 error includes statistical error and error in modeling calibration and variable temperature blackbody radiance.
- Best results for high responsivity region below 1350 cm-1

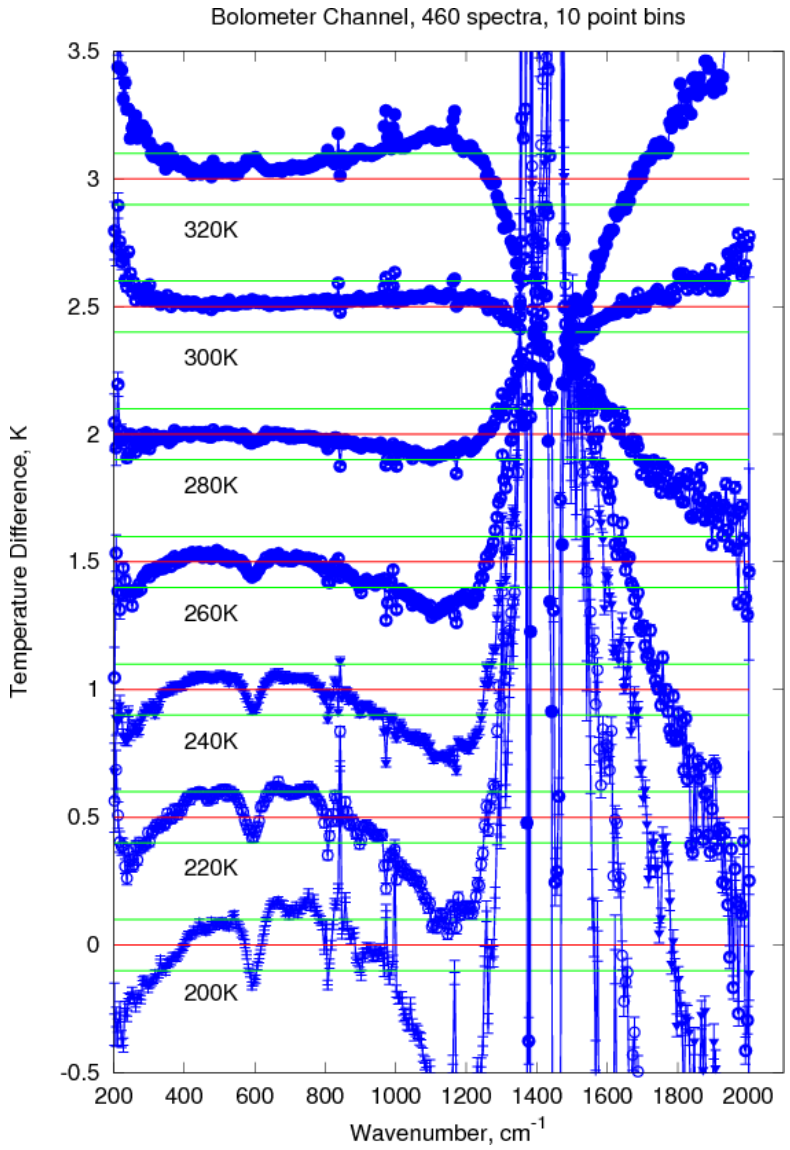

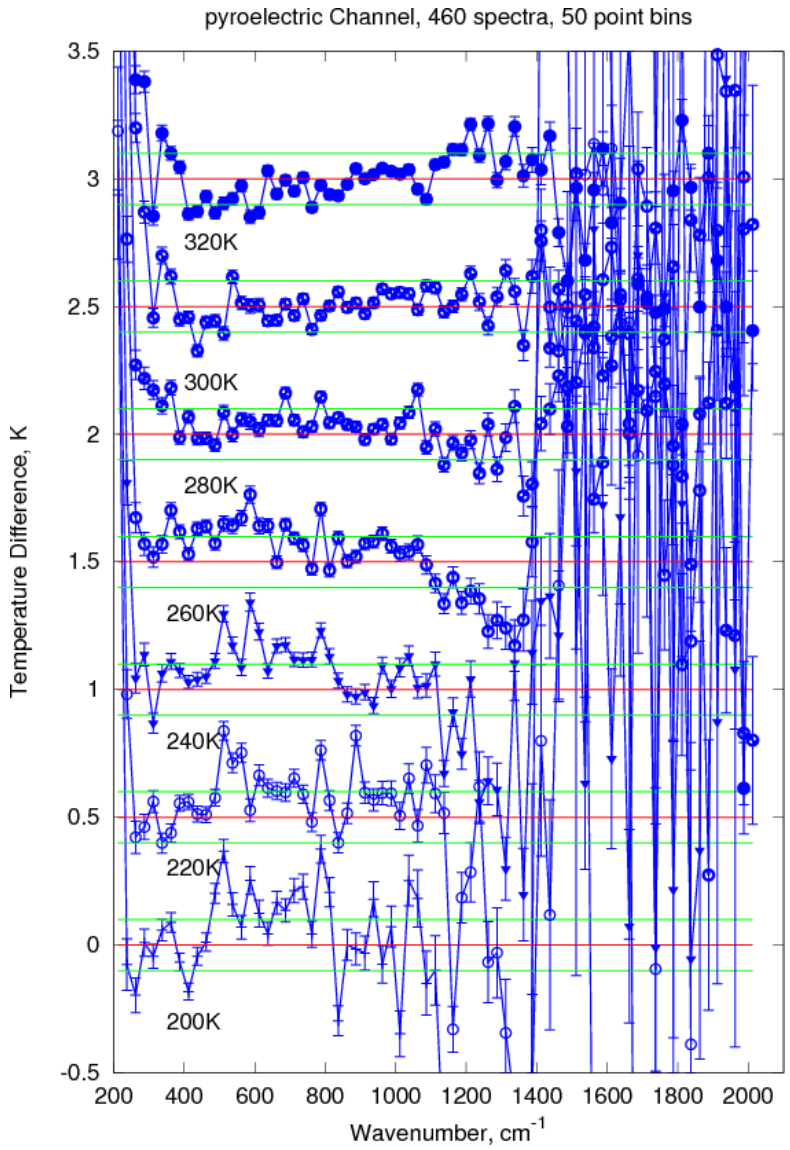

Comments and Observations

- We use single detectors to cover the entire thermal spectrum, so:
  - Small nonlinearities will alias radiance from the blackbody peak to other parts of the observed spectrum;
  - Real and Imaginary bolometer radiance differences show this
  - Using separate detectors to cover the shortwave part of the spectrum (as in the CLARREO mission concept design) will reduce the consequences by reducing the required dynamic range and putting aliased power out-of-band.
- For the tested range of 200K to 320K scene temperature, over the spectral range 250-1350 cm-1 where responsivity for both channels is high:
  - Radiance bias is generally less than 0.00015 W/m^2 sr cm^{-1};
  - Brightness temperature bias is generally less than 0.2K;
  - Bolometer bias is dominated by uncorrected nonlinearity;
  - There may still be a source of bias in the pyroelectric channel that is not yet accounted for.